Paleomagnetic Results from the Singhbhum Craton, India: Remagnetization, Demagnetization, and Complication

Anthony F. Pivarunas[1*], Joseph G. Meert[1], Karastin D. Katusin[1], Manoj K. Pandit[2], Scott R. Miller[1], Aubrey Craver[1], Kelli M. Roderus[1], Anup Sinha[3]

[1]University of Florida, Department of Geological Sciences, 241 Williamson Hall, Gainesville, FL 32611
[2]Department of Geology, University of Rajasthan, Jaipur, Rajasthan India.
[3]Geomagnetic Research Laboratory, Regional Center of Indian Institute of Geomagnetism, Allahabad, 221 505, India.
*corresponding author is now at the United States Geological Survey, apivarunas@usgs.gov

Abstract

We report a complicated magnetic fidelity through time in Singhbhum Craton, India, with new, geographically wide-spread and spatially detailed, paleomagnetic results. The Singhbhum Craton in eastern India is cross-cut by multiple generations of the so-called "Newer Dolerite" dykes. A previously published 1765 Ma paleomagnetic pole represents a useful constraint on the Singhbhum Craton during the amalgamation of the Columbia supercontinent whereas an older ~2763 Ma paleomagnetic pole is problematic. We present additional data from the 1765 Ma dykes that results in a grand mean paleomagnetic pole at 43°N, 320°E (A95=11°, K=17; N=13). The 1765 Ma pole is supported by a positive baked contact test. Our additional data shows that paleomagnetic results from the 1765 Ma dykes are more complicated by magnetic overprints than originally reported. We also argue that the steep inclination paleomagnetic data from the Singhbhum Craton, previously assumed to represent a Neoarchean signal, are part of a complicated group whose magnetic age is uncertain. We establish a minimum age of 2250 Ma for connecting the Singhbhum and Dharwar cratons on the basis of published geochronology and our interpretation of paleomagnetic data in this paper. Paleomagnetic data from both cratons can be juxtaposed using a simple Euler pole rotation of the Singhbhum Craton relative to Dharwar.

1. Introduction

Untangling the paleomagnetic record of geologic terranes with complex tectonothermal histories is a difficult endeavor since primary magnetic signatures may become altered. Peninsular India – the Dharwar, Bastar, Singhbhum, Bundelkhand, and Aravalli cratons along with the Banded Gneiss Complex (BGC) – has a substantial history of growth and deformation, beginning in the Eoarchean (Naqvi and Rogers, 1987; Ramakrishnan and Vaidyanathan, 2008; Meert and Pandit, 2015, Jain et al., 2020, Jayananda et al., 2020). Typical for Archean cratons (Halls, 2008), these nuclei are cut by numerous mafic dykes. A concerted effort to precisely date the many generations of mafic dykes has yielded a wealth of robust geochronologic data in the Dharwar (Halls, 2007; Belica et al., 2014; Kumar et al., 2015; Nagaraju et al., 2018a; Pivarunas et al., 2019; Nagaraju et al., 2018b; Söderlund et al., 2019 and references therein), Bastar (French et al., 2008; Pisarevsky et al., 2013; Shellnutt et al., 2018), Singhbhum (Kumar et al., 2017; Shankar et al., 2017; Srivastava et al., 2019), and Bundelkhand (Pradhan et al., 2012) nuclei. In concert with knowledge of dyke ages, proof for the time of magnetization acquisition – determined by such means as the 'baked contact test' of Everitt and Clegg, (1962) for intrusions – are of paramount importance to paleomagnetic studies. Otherwise, the correlations between continental blocks or inferences of movement are premature at best and spurious at worst. The protracted Precambrian intrusive history of Peninsular India, restricted within a finite amount of space, creates complexities in the evaluation of paleomagnetic data from dykes (Pivarunas et al., 2019).

The five major nuclei that comprise Peninsular India can be divided into a North Indian Block (NIB) (Aravalli-Banded Gneiss Complex, Bundelkhand, and Marwar region) and a South Indian Block (SIB) (Dharwar, Bastar, Singhbhum), separated by the roughly east-west trending Central Indian Tectonic Zone (CITZ) (Fig. 1). The 1.6– 1.5 Ga activity has been recently argued (Bhowmik, 2019) to represent early quasi-assembly of the NIB and SIB (accretional orogeny) and the major Stenian-Tonian (1.1-1.0 Ga) aged tectonothermal event resulted from full assembly of the SIB and NIB during a Himalayan-type orogenic pulse. Paleomagnetic data from the NIB (Miller and Hargraves, 1996; Gregory et al., 2006; Malone et al., 2008; Pradhan et al., 2010) and SIB (Venkateshwarlu and Chalapathi-Rao, 2013) support SIB-NIB assembly by 1.1-0.9 Ga, although coeval data from the intervening time are lacking and therefore this should be regarded as the minimum age of assembly.

Paleomagnetic data from both the Dharwar Craton and the northern block of the Southern Granulite Terrain (SGT) demonstrate that they were contiguous since at least 2367 Ma (Halls et al., 2007; Belica et al., 2014; Dash et al., 2013; Pivarunas et al., 2019), while geochronologic considerations (Meissner et al., 2002; Clark et al., 2009) suggest these areas were conjoined as early as ca. 2500 Ma (see also Meert et al., 2010). A 2367 Ma dyke from the Bastar Craton (Liao et al., 2019) tentatively supports an early amalgamation of Bastar and Dharwar. Stronger evidence for their unity is derived from 1888 Ma dykes from the Dharwar and Bastar cratons (French et al., 2008; Meert et al., 2011; Belica et al., 2014; Radhakrishna et al., 2013), although an earlier amalgamation (Rajesham et al., 1993; Santosh et al., 2004) and a later quasi-separation (Santosh et al., 2004) are proposed.

The Singhbhum nucleus and its direct neighbor, Bastar Craton were canonically considered as adjacent partners, since the Neoarchean, on the basis of indirect evidence. Their hypothesized connection in the Neoarchean is supported by a semi-continuous gneissic fabric (Chetty, 2014), an approximate age match – based on a problematic 2.7 Ga Sm-Nd 'isochron' – of dyke swarms from Bastar Craton (Srivastava et al., 2009) and from Singhbhum Craton (Kumar et al., 2017), and tradition (Meert et al., 2011; Basu and Bickford, 2015). The Singhbhum/Dharwar cratonic nuclei synchronously hosted 2250 Ma (Demirer, 2012; Srivastava et al., 2019) and 1790-1760 Ma (Demirer, 2012; Shankar et al., 2017; Söderlund et al., 2019) dyke intrusions. While similar 'bar-code' pattern (Bleeker and Ernst, 2006) ages of intrusions is considered a strong indicator of unity, geochronological data sans coeval paleomagnetic data excludes rigorous tests of such age-based reconstructions.

Here, we present new, geographically widespread paleomagnetic data from a wide array of dykes from Singhbhum Craton. The purpose of our study is to (i) add to the paleomagnetic database from Singhbhum Craton; (ii) test the reliability of previously published results from the Singhbhum Craton; (iii) identify additional paleomagnetic data from the Singhbhum Craton; (iv) use these data to assess the contiguity of the NIB/SIB and (v) compare the data to the global paleomagnetic database.

2. Geological Overview

The 40,000 km^2 Singhbhum Craton is the northernmost terrane of the South Indian Block. The Singhbhum Craton is bordered to the north by the Chhotanagpur Granite-Gneiss Complex (Mukherjee et al., 2017). The southern border of the Singhbhum Craton is demarcated by the Mahanadi Rift, separating it from the Bastar Craton to the southwest, and older Rengali Province granodiorite gneisses and supracrustal rocks of the Eastern Ghats orogenic belt, to the southeast (Sharma, 2009). Recent reviews of Singhbhum Craton genesis and evolution provide details of the cratonic framework geology (Olierook et al., 2019; Pandey et al., 2019; Chaudhuri et al., 2020); we recommend these works for those looking for a synoptic view of the craton architecture.

Singhbhum Craton comprises four major litho-stratigraphic units, viz. the Older Metamorphic Group (OMG), Older Metamorphic Tonalite Gneisses (OMTG), Iron Ore Group (IOG), and Singhbhum Granite complex, that yield Paleoarchean ages (Chaudhuri, 2020). Xenocrystic zircons within the OMTG, detrital zircons within the Mahagiri Quartzite, and a detrital zircon within modern sediment have preserved a Hadean to Eoarchean signal (Mukhopadhyay et al., 2014; Chaudhuri et al., 2018; Miller et al., 2018; Sreenivas et al., 2019). A dacitic lava tuff interbedded with quartzite and banded iron formations in the Southern IOG yielded an age of 3506.8 ± 2.3 Ma (Mukhopadhyay et al., 2008) and represents the oldest dated igneous event in the Singhbhum Craton. An even older event is hinted at in a 3527 ± 17 Ma U-Pb zircon age from a TTG gneiss in the northeast of Singhbhum Craton (Acharyya et al., 2010). The Singhbhum Granite complex dominates the central region (Fig. 1) and was built in pulses from 3.38-3.25 Ga (Upadhayay et al., 2019; Dey et al., 2017; Dey et al., 2020). The metasedimentary rocks and amphibolites of the OMG and the tonalite-trondhjemite gneisses of the OMTG occur as small enclaves within the Singhbhum Granite. The Iron Ore Group includes three volcano-sedimentary basins surrounding the east, south, and west sides of the Singhbhum Granite Complex. Secondary units such as

Dhanjori Volcanics and Simlipal Group were emplaced over the cratonic nuclei from Mesoarchean to Neoarchean (Misra and Johnson, 2005; Singh et al., 2021).

The Archean lithologies of Singhbhum Craton, particularly the Singhbhum Granite (Fig. 1), are cut by a dense array of dykes known as the 'Newer Dolerites'. Until recently, the emplacement ages for the Newer Dolerites were limited to poorly constrained K-Ar system ages yielding ages ranging between 2200-900 Ma (Naqvi and Rogers, 1987; Srivastava et al, 2000; Bose, 2008). More precise geochronology (Pb-Pb baddeleyite) identified at least four episodes of Newer Dolerite intrusions at 2800 Ma, ~2760 Ma (Kumar et al., 2017), ~2260 Ma (Srivastava et al., 2019), and ~1765 Ma (Shankar et al., 2014, 2017). Srivastava et al. (2019) separate the Newer Dolerites into as many as 7 swarms based on the four precise ages as well as cross-cutting relationships inferred from satellite imagery. Inherent to this approach is an assumption that dyke trends are diagnostic for age. This is a good first-order approximation, given the difficulties of sampling every single dyke in a craton for geochronology; however, we emphasize that dykes from the same intrusive event may have multiple trends (Samal et al., 2015).

The densely concentrated Newer Dolerite dyke swarms intruding the Singhbhum basement rocks are predominately mafic with subordinate ultramafic and intermediate compositions (Mir and Alvi, 2019). The mafic dyke geochemistry ranges from tholeiitic to alkalic (Srivastava, 2000; Bose, 2008; Mir et al., 2011; Dasgupta, 2019). The width of individual dykes ranges from ~1-70 m, with small dykelets regularly off-shooting main dykes (Mir et al., 2011; Katusin, 2017). Larger dykes define two main cross-cutting trends, oriented either N-S to NNE-SSW or NW-SE to WNW-ESE (Meert et al., 2010; Mir et al., 2011). Our field observations indicate that the northerly-trending dykes are generally relatively older when cross-cutting relationships can be observed. Large dykes have subvertical orientations, some dykes <1 m in width at Bhima Kunda are not vertically emplaced. However, larger dykes (>1 m width) dykes at Bhima Kunda are clearly vertical.

2.1 Previous Paleomagnetic Work

An early paleomagnetic study of the Newer Dolerite swarm (Verma and Prasad, 1974) used rudimentary low-temperature thermal magnetic cleaning that revealed three groupings (N.D. 1-3) of directional paleomagnetic data. Other paleomagnetic studies were conducted on rocks of the Iron Ore Group by Kumar and Bhalla (1984) and Das et al. (1996). Recent paleomagnetic work on the Singhbhum Craton focused on precisely dated mafic dykes (Shankar et al., 2017; Kumar et al., 2017). Two WNW-trending dykes were dated to 1765.3 ± 1.0 Ma (Shankar et al., 2014). After stepwise demagnetization, the authors reported a consistent northwesterly-directed negative shallow remanence with a mean direction of D= 329°, I= -23° (k =32, α_{95}= 9°, N= 9 dykes). This is broadly consistent with one of the directions identified in low-temperature results of Verma and Prasad (1974). In the Shankar et al. (2017) study, sizeable secondary components of magnetization were often removed, but not discussed in any detail (see

Figure 3 of that manuscript). The mean characteristic direction was supported by a baked contact test from a dyke which paralleled the dated dyke. Shankar et al. (2017) reported a paleomagnetic pole at 45° N, 311° E (A95 = 7°). The reliability factor assigned to that study is R = 6 (Meert et al., 2020) and therefore is considered as a "key" paleopole at 1765 Ma.

Kumar et al. (2017) confirmed the absolute age of older, NNE-SSW trending dykes, in the Singhbhum Craton based on well-constrained Pb-Pb baddeleyite ages yielding an average of 2762.4 ± 2.0 Ma. Distinctly older and younger ages were also identified in that study (~2800 Ma and ~2752 Ma), although the younger age may simply represent protracted dyke emplacement, as is seen in the Dharwar Craton and SGT. Stepwise demagnetization revealed a steep, dual polarity remanence that is consistent with results from the limited study by Verma and Prasad (1974). Kumar et al. (2017) argued that a reversal test with an "R_c" classification (McFadden and McElhinny, 1990; hereafter MM1990) was evidence of a primary magnetization. We recalculated their test using a correct form of the MM1990 reversals test which yielded an "indeterminate" result. We also applied a modified Bayesian reversals test (Heslop and Roberts, 2018) which yielded "positive support" for the hypothesis of a common mean between the antipodal directions. The mean direction is D=226°, I=+84° (α_{95}=6°; N=14) with a corresponding paleomagnetic pole at 14° N, 78° E (A95 =11°; Q=6).

3. Methods

A total of 96 sites (468 directly drilled samples along with 84 block samples) from 84 dykes were collected throughout the northern and southern Singhbhum Craton over the course of three field seasons (Fig. 2). Paleomagnetic sites from this study are geographically concentrated south of Jamshedpur in the northern Singhbhum Craton, and east of Keonjhar in the southern Singhbhum Craton (Fig. 2). Sampling was targeted on unambiguously *in-situ* dyke outcrops, typically in rivers or recent road cuts due to deep tropical weathering in the area. Samples were also collected from host rocks – granites and gneisses – at sites suitable for baked contact tests (18 sites). Baked contact tests had a low rate of success due to weak or unstable magnetizations within the host rocks. Paleomagnetic samples were collected in the field with a water-cooled, gasoline-powered drill and oriented with both a magnetic and a sun compass. Oriented hand samples were taken where drilling was unfeasible or when equipment failures occurred.

Samples were returned to the University of Florida where they were trimmed to a standard size (after drilling, in the case of oriented hand samples). Natural remanent magnetization (NRM) directions were measured using either a Molspin spinner magnetometer or a 2G-77R cryogenic magnetometer. Two pilot specimens (from the same sample) from each sampling site were demagnetized by thermal and alternating field (AF) methods using either an ASC TD-48 thermal demagnetizer, homebuilt AF demagnetization apparatus, or DTech 2000 AF demagnetizer. Subsequent demagnetization procedures were optimized based on pilot sample behavior. Generally, multiple specimens from each site were demagnetized using both methods. Selected samples were subjected to both thermal and AF demagnetization to more fully characterize their response. After complete demagnetization, paleomagnetic vector directions were recovered with principal component analysis (Kirschvink, 1980) or great-circle analysis, using IAPD software (Torsvik et al., 2016). Within-site analyses and statistical analyses of directions (Fisher et al., 1953) were conducted using both IAPD and the PmagPy software package (Tauxe et al., 2016). Susceptibility and temperature-dependent susceptibility were measured from samples at selected sites with a KLY-3S Kappabridge with a CS-3 furnace attachment in order to characterize magnetic behavior and signal carriers in the samples.

4. Results

Stable paleomagnetic directional data were recovered from a total of 59 individual cooling units (72 individual sites). In the following discussion, we highlight the fact that some sites were sampled multiple times during this investigation. In an effort to help clarify our sampling, note that each site is preceded by IXX where XX represents the last two digits of the year in which the samples were collected (i.e. I14xx samples were collected in 2014, I16xx in 2016 and I17xx in 2017). These sites included directly dated dykes ranging in age from 2800 Ma to 1765 Ma. Two sites (I1417 and I1733) were sampled from a 2800 Ma dyke. Another site (I1713) was sampled from a 2763 Ma dyke, and multiple sites (I1637, I171, I1722) were taken along the large WNW-trending 1765 Ma dyke. Sites were rejected for typical reasons in paleomagnetic studies: random directional data (causes include unstable magnetic behavior or lightning strikes), evidence of intra-outcrop rotations, or too few (1 or 2) stable samples for meaningful statistics.

4.1 Results from 1765 Ma dyke swarm

We isolated a characteristic northwest-declination, shallow up-inclination magnetization (Fig. 3) in 9 dykes (12 sites) in Singhbhum Craton (Fig. 3a; Table 2). This direction is typically resolved after the removal of low-medium blocking temperature/coercivity secondary components (Fig. 3b). Curie temperature analyses show that this remanence is carried by magnetite (Fig. 3c). This magnetic direction is sometimes almost completely overprinted by other magnetic components. Two large WNW-trending dykes (sites SKJ10 and SKJ15; Shankar et al., 2014) were directly dated to 1765 Ma. Subsequent paleomagnetic work (Shankar et al., 2017) identified the northwest-declination, shallow up-inclination paleomagnetic direction in the dated dyke (SKJ10) and other dykes throughout the Singhbhum Craton.

The characteristic NW-up remanence was isolated in these dykes after the removal of secondary steep magnetic components, although the remagnetization was sometimes complete along the margins of the dyke (Figs. 4,5). Great-circle analysis was required in several cases to determine a mean direction (e.g. I147, I1637, I171, I1729). A mean direction for the 1765 Ma dykes was calculated by combining our results and those of Shankar et al. (2017). The result is based on 183 samples from 13 sites (9 cooling units) with a mean declination=321.6º, inclination=-15.7º (a95=12.9º, k=17.2) with a resultant paleomagnetic pole at 43.2 N, 319.9 E.

We attempted a baked contact test at a small northerly-trending dyke (site I172) near the Khanjhari Reservoir that is cross-cut by a large, WNW-trending dyke previously dated to 1765 Ma (sites I1637+I171+I1722+K10+SKJ10; Shankar et al., 2014, 2017) (Fig. 4). After the removal of random low-temperature/coercivity components, a consistent paleomagnetic remanence was found within the N-S trending dyke (I172) near the contact with the WNW trending dyke (I171) with a mean direction of D= 330°, I= -18° (k=174, α_{95}=3.5°, n=11). Two samples from the granite immediately adjacent (3 cm from contact) to the dyke yield a similar paleomagnetic direction of D= 327°, I= -27°. Further away from both I171 and I172 (~2-3 m), two samples of granite preserve a distinctly different direction at D= 358°, I= +20°; one preserving also a low-coercivity NW-shallow overprint (D= 337°, I= -41°). This illustrates the complexity of this particular baked contact test. Based on cross-cutting relationships, the northerly trending dyke I172 is older and was likely partially reset along with some of the granitic material during the intrusion of the younger 1765 Ma dyke. Further complications arise from the fact that we isolate a NE-up overprint in the younger dyke (Fig. 4). The NE-directed component is not fully removed using thermal demagnetization; however, AF-demagnetization is effective at resolving the characteristic NW-up direction (Fig. 4d). In some samples, high-temperature thermal demagnetization was followed by AF demagnetization, revealing a characteristic NW-shallow up direction statistically similar to the mean direction obtained by Shankar et al. (2017) (Fig. 3). These repeated trajectories from northeast directions to northwest directions illustrate that the NE-direction is a persistent overprint (Supplementary Section 5). This alteration of paleomagnetic directions is particularly pronounced along the margins of the dyke. Our interpretation is that the 1765 Ma dyke remagnetized the older northerly trending dyke and at least some of the country rock within the baked zone. Subsequently, a NE-shallow magnetization overprinted the margins of the larger dyke.

In an effort to resolve this conundrum, we collected samples at a second site along the same large dated dyke (site I1722) that corresponds to site SKJ10 of Shankar et al. (2017). They reported separate means for site SKJ10 and site K10 although both are from the same large dyke. Our analysis showed similar magnetic behavior, a trend revealed by AF demagnetization from a northeasterly-shallow to a northwesterly, shallow paleomagnetic direction (cf. Fig. 3 of Shankar et al., 2017). We combine magnetic vectors isolated at different sites (I1637, I171, I172, I1722, K10, SKJ10) by AF demagnetization, thermal demagnetization, and great circle analysis to calculate a new mean direction for this dyke as a single cooling unit: D= 327°, I= -17° (k=65.8; α_{95}=11.4°; N=6 sites; n=48 samples).

Previous work indicated a positive baked contact test at a WNW-trending dyke (our site I176; Fig. 5) (K12; Shankar et al., 2017). This dyke is a few kilometers northeast of site I172 and the Khanjhari

Reservoir. We resampled this dyke with a detailed drilled sampling profile across the dyke interior, margin, and baked host rocks in order to supplement the previous hand-sample collection and determine the full width of the baked zone. Samples from the coarse-grained interior of the dyke contained a southwest-directed, intermediate, down-inclination direction, D=235°, I= +63° (k=27, α_{95}=8°) that was removed between 525 and 580 °C or between 5 and 15 mT. After removal of this component, a stable NW-shallow up-inclination component was recovered with D=348°, I= -20° (k=18, α_{95}=14°). Thermally demagnetized samples from the dyke margin behaved differently from those in the dyke interior and yielded a mean direction at D=193°, I=+80° (k=17, α_{95}=15°). One sample (number 8) at the contact showed different specimen behavior under different demagnetization treatments, with univectorial thermal decay defining a steep component (D/I: 113°/+89°), while AF demagnetization yielded a shallow component (D/I: 338°/-9°) after the removal of a low-coercivity steep component similar to the direction in the dyke interior (similar behavior is apparent in Figure 3 of Shankar et al., 2017). Individual samples of granite yielded random directions. Therefore, considering both the complex paleomagnetic behavior at the contact and our ungrouped results from the granite, we cannot confirm the earlier baked contact test here. Typically, the fine-grained margins of dykes are viewed as better magnetic recorders than the interiors (Halls, 2008), but this situation is inverted at this dyke. To further complicate the signal in the WNW-trending dykes, we identify additional overprints along the margins of sites I176 (Fig. 6), I1720, and I1734 . However, we emphasize that these overprints are *secondary* to the NW-shallow up component. The thermal effects of the NW-shallow magnetization extend to other dykes within the Craton. We have isolated the NW-shallow up direction (or its antipodal direction) as an overprint on 12 other dykes (87 samples). These overprints are commonly discovered in samples with pyrrhotite (components removed by 350°C). The mean direction of the dual-polarity overprint is Dec=327.5, Inc=-6.8 (k=10.4, a95=14.1) with a resultant paleopole at 49.5 N, 321.8 E. The mean pole and direction overlaps with the 1765 Ma dyke pole.

We posit the following arguments in favor of a primary NW-shallowly directed magnetization in the 1765 Ma dykes. (1) The direction isolated in the dated dyke (SKJ10) is identical to directions observed in other dykes that follow the WNW trend. (2) Although we were unable to duplicate the baked contact test reported in Shankar et al. (2017), the baked contact test reported in that study stands. (3) Magnetic directions at cross-cutting dykes I171 (younger) and I172 (older) are consistent with the hypothesis that I171 baked I172, although the baked contact test was not ideal. (4) There is a widespread dual polarity NW-up/SE-down overprint on many older dykes in the region (12 dykes, 83 samples). (5) The NW-shallow up direction is sometimes overprinted by younger magnetizations particularly along altered margins of the dykes. (6) The pole averages secular variation according to the Deenen et al. (2011, 2014) parameters with our $A95_{min}$= 4.3° < $A95_{1765}$=12.9° < $A95_{max}$=16.3°.(7). At present, the presumed 1765 Ma magnetization resembles no younger poles in the Singhbhum craton. Our evaluation of this pole using the R-value (a measure of the 'quality' of a particular paleomagnetic result, see Meert et al., 2020) yields an R-value of 6 (with baked contact test marked as $R4_{Co}$). The pole lacks a reversals test; however, the overprint directions on other dykes are of dual-polarity. On the basis of this evidence and reasoning, we conclude a 1765 Ma primary NW-shallow magnetization exists in the craton.

4.2 Steeply-inclined dual polarity magnetic data

Within the Singhbhum craton, there are at least 4 distinct moderate to steeply inclined directions that were isolated in our study; hereafter referred to as Singhbhum Paleomagnetic Groups 1-4 (SPG1-4; Fig. 7). Forty-three cooling units (53 sites) have paleomagnetic directions that are within these confines (Table 3). Typically, strong trend-directional affinities are not recovered, which indicates either a given dyke swarm was emplaced along multiple trends, or some magnetic signals of older dykes were reset.

The moderately-to-steeply-inclined magnetizations were isolated in Neoarchean and other north-northeast-trending dykes (see Kumar et al., 2017; Fig. 7). They were also isolated in west-northwest-trending dykes, baked and unbaked granites, and altered exterior margins of younger (1765 Ma) dykes (Figs. 5,6). Thus, it is likely that at least some of the steeply inclinded directions represent remagnetizations that are younger than 1765 Ma. This clearly indicates that dual-polarity, intermediate-steep inclination magnetizations in Singhbhum Craton are a group of varied origin, leading to our framework of multiple groupings.

The characteristic magnetic components from these dykes were isolated at a wide range of temperatures and coercivities (Figs. 8,9). Lower unblocking-temperature/coercivity components were typically present. The remanence of dykes with intermediate-steep dual-polarity paleomagnetic directions are predominately carried by magnetite (Fig. 8e), although some dykes exhibit different rock magnetic properties. The majority of susceptibility-temperature experiments are non-reversible and indicate growth of a new magnetic phase during heating-cooling cycles (Fig. 8e).

4.2.1 Singhbhum Paleomagnetic Group 1 (SPG1)

Paleomagnetic results from 19 dykes (24 sites) in Singhbhum Craton fall into a dual-polarity group (SPG1; Table 3a; Fig 8a,b) with either NE-steeply down or SW-steeply up magnetic vectors (Fig. 7). These dykes have both NNE and NW-trends. After inverting the NE-down directions, we obtain a mean direction at D= 218°, I= -77° (k= 41, α_{95}= 5.3°; N=19).

We performed a baked contact test at site I1427 on a small (5 m wide) WNW-trending dyke in the southern Singhbhum Craton (Fig. 10a). Samples from the dyke showed a consistent univectorial direction of D= 66°, I= +78° (α_{95}=8°). Samples at the contact, including some mixed dyke/granite specimens yielded a mean direction of D= 255°, I= +87° (α_{95}= 15°). Unbaked samples yielded a mean D= 288°, I= +79° (α_{95}= 8°). Due to the steep inclinations, this baked contact test is more difficult to interpret; however, the mean dyke and unbaked directions are statistically distinct which is supportive of a primary magnetic signal, although it does not constitute an ideal positive baked contact test. A susceptibility profile across the dyke does not show indications of baking along the margins as all contact samples have similar susceptibilities (Supplementary Material). The significance of this baked contact test is uncertain because the direction from the 'unbaked' granite samples is similar to the 'primary' Neoarchean remanence in the NNE-trending dykes (Kumar et al., 2017).

The complexities associated with the SPG1 directions are further illustrated in two cross-cutting dykes at Bhima Kunda along the Baitarani River. At sites I1647 and I717 (both on a 0.75m wide, NE-trending dyke), three components of magnetization were isolated (Fig. 11a). Near the contact with a NW-trending dyke (I1646, 0.75m wide), samples show a univectorial southwest-directed, steep-up magnetization (SW-up; Fig 11b, c). A sample, collected about 35 cm from this contact on the NE-trending dyke (site I717, sample 3b), shows a low-coercivity overprint (SW-steep up; Fig. 11b,d) and a higher coercivity component that is roughly antipodal (NE-steep down; Fig. 11b,d). Samples away from the 'baked zone' (I1717, 2.5 m) show a NE-steep down high temperature component that is overprinted by a NW-shallow up component similar to the 1765 Ma direction (Fig. 11b,e). Samples from this dyke appear to show an ideal baked contact test including evidence for a hybrid zone in sample 3b. Unfortunately, data from the cross-cutting dyke show a high temperature/coercivity component that is of the opposite polarity as discussed below.

Samples from the NW-trending dyke (I1646) show the NE-steep down direction with NW-shallow overprints (Fig. 11b,f). The NE-steeply down component in I1646 is antipodal to the directions observed at the contact between the two dykes, but matches the high-temperature/coercivity component away from the contact in both dykes. Currently we have no unequivocal explanation for the apparently 'reverse' direction in samples immediately adjacent to the contact zone; however, the SPG1 direction pre-dates 1765 Ma, as both dykes are overprinted by the NW-shallow up direction. Intra-dyke reversals were previously reported by Liebke et al. (2010, 2012), but the spatial arrangement, as shown in Figure 11, renders this explanation untenable for these relatively small dykes.

In spite of the equivocal baked contact tests cited above, we believe that the SPG1 magnetization is older than 1765 Ma and may be primary. The mean downward-directed direction is D=51.5°, I= +76.4° (k=49.5, α_{95}= 5.7°; N=14) and the mean upward-directed direction is D=179.9° I= -75.6° (k=42.3, α_{95}= 11.9°; N=5). This dual polarity magnetization passes the reversal test with a grade of "C" (McFadden and McElhinny, 1990). The paleomagnetic pole, calculated from the mean of VGP's, falls at 40.2 N, 104.6 E (K=13.4, A95=9.5) and averages secular variation based on the Deenen et al. (2011, 2014) parameters ($A95_{min}$=3.7°, $A95_{max}$=12.8°).

4.2.2 Singhbhum Paleomagnetic Group 2 (SPG2)

Paleomagnetic data from 13 dykes within Singhbhum Craton have steep magnetic inclinations of dual polarity that are distinct from the steep SPG1 directions (Table 3b; SPG2; Fig 8,c,d). The down-inclinations data cluster in the southwest-quadrant, with antipodal, up-inclination directions in the northeast (Fig. 7). Our mean direction (after reversing the negative inclination results) falls at D= 201°, I= +80° (k= 35, α_{95}= 7°). These data closely resemble results from the Neoarchean dykes reported in previous studies (Verma and Prasad, 1973; Kumar et al., 2017). The majority of our studied dykes have an NNE-trend, in agreement with the arguments put forth by Kumar et al (2017).

A baked contact test was conducted on a 9-meter wide, northerly-trending dyke (site I178), parallel to sites K7 (Kumar et al., 2017) and I177 (our study). We sampled site I178 (the parallel dyke ~100 meters to the east), because of the favorable, sharp, and exposed dolerite-granite contact (Fig. 10b). Samples from the interior and exterior parts of the dyke were consistent under both thermal and alternating field demagnetization, with a well-defined mean direction D=188°, I= +68° (k= 20, α_{95}= 9°). Samples from the baked and unbaked granite yielded a mean direction at D=205°, I= +63° (k=16, α_{95}=24°; Fig. 8b) similar to the dyke. This baked contact test is therefore negative. Interestingly, the characteristic dyke direction is antipodal to the mean direction from the northerly-trending dyke, just to the west (K7+I177: D= 012°, I= -67°; k = 806, α_{95}= 8.8°).

The SPG2 magnetization is similar to overprints on the 1765 Ma dykes and therefore post-dates 1765 Ma (Fig. 6). Along with the negative baked contact test at site I178, the evidence does not support a primary Neoarchean paleomagnetic signal. However, certain dykes within the group (such as I1636, undated but cut by a 1765 Ma dyke), have secondary directions which roughly correspond with the 1765 Ma event. This indicates that some magnetizations in this group were acquired *before* 1765 Ma, but not necessarily in the Neoarchean.

Due to the similarity between SPG2 and results of Kumar et al. (2017), we combine both these data to reach a grand mean direction of Dec=206.2°, Inc=+81.8° (k=47.5, α_{95}= 4.3°; N=24 dykes). Sites K7 and K9 of Kumar et al. (2017) were combined with our sites I177 and I1713 (as single cooling units). We eliminated site Q (Verma and Prasad, 1972) that was included in the Kumar et al. (2017) analysis. The mean paleomagnetic pole for SPG2 and Kumar et al. (2017) falls at 7.9° N, 79.2° E (K=15, A95=8.0°). With our added data, the pole has a positive reversal test with a grade of "C" (McFadden and McElhinny, 1990), and has averaged secular variation based on the Deenen et al. (2014) parameters ($A95_{min}$=4.8°, $A95_{max}$=11.1°)

4.2.3 Singhbhum Paleomagnetic Group 3 (SPG3)

Paleomagnetic data for 6 dykes (10 sites) exhibit an easterly-up/westerly-down intermediate-inclination dual-polarity paleomagnetic direction (SPG3; Figure 9; Table 3c). We combine several sites from a ~10 m thick WNW-trending dyke at Bhima Kunda (I1435, I1642, I1644, I1714, I1715) in reporting this mean direction as they represent a single cooling unit. The mean direction from these dykes falls at D= 89.9°, I= -48.4° (k= 28, α_{95}= 13°). This direction was isolated either after removal of a low-medium temperature/low coercivity overprint (site I1730) or isolated as a single component (site I1635) (Fig. 9). Demagnetization and rock magnetic experiments indicate that this remanence is carried by magnetite (Fig. 9). Dykes with this direction are mostly northeast-trending, although a single dyke exposed in the Bhima Kunda river section trends northwest.

The largest dyke (sites I1642, I1644, I1714, I1715) at the Bhima Kunda river section provides constraints on the age of this magnetization. The contact gneiss is cut by cm-scale dykelets, as well as a larger apophysis (site I1644) which we also sampled. All sampling areas carry a substantial overprint with a mean at D=356°, I=+12° (k=24, α_{95}=10°). This direction was isolated at temperatures up to 400 °C. The only stable magnetization isolated in the gneissic rocks adjacent to the dyke is antipodal to this overprint (samples 9 and 10 from site I1642). After removal of the overprint, the characteristic easterly, intermediate-up-inclination component was isolated from the dyke (sites I1642, I1714) and apophysis (I1644) with a mean at D=100°, I=-46° (k=33, α_{95}=5°). This component was persisted to temperatures up to 545°C. AF demagnetization was more successful in isolating this component.

A detailed sampling profile (I1715) examined the relationship between the 'large' Bhima Kunda dyke (described above) and a smaller, more northwesterly-trending dyke ('bridge' dyke; sites I1436, I1643) (Fig. 12, Supp. Fig 1). The two dykes coalesce just before an abrupt hillslope where cross-cutting relationships are obscured. Each dyke has a unique paleomagnetic direction, away from the intrusive contact (i.e. 'far-field ChRMs'). The interior of the smaller bridge dyke yields a high-temperature component with a mean D=261°, I=-45° (k=46, α_{95}=14°).

Samples were drilled at the intersection of the two dykes (Fig. 12). Samples from both dykes show a persistent (medium to high temperature) overprint mean at D=334°, I=+35 ° (k=10, α_{95}=12°; Fig. 12). The characteristic remanence of both dykes at their intrusive contact is an easterly, intermediate up-polarity direction (D=103°, I=-46°; k=17, α_{95}=13° 'large dyke') and a D=105°, I=-37°; k=25, α_{95}=11°) for the 'bridge dyke'). These directions are also identical to the primary signal ~150 m away on a WNW-trending ('large') dyke at sites I1642, I1644 and I1714. That the consistent east, moderate-up-inclination direction is seen in *both* dykes suggests that the WNW-trending ('large') dyke cut and baked the NW-trending ('bridge') dyke. The survival of this remanence at the intrusive contact along with a distinct paleomagnetic direction preserved in the dykes farther away, supports a positive baked contact test on the E-up direction as well as an inverse baked contact test on the W-up direction.

The absolute age of this magnetic component is uncertain; however, the baked contact test suggest it is a primary signal. The virtual geomagnetic pole calculated from this mean direction falls at 10° S, 204°E (K = 19; A95=16°). This represents a small sampling of dykes from around Singhbhum Craton and requires more data to ensure that it has averaged secular variation.

4.2.4 Singhbhum Paleomagnetic Group 4 (SPG4)

Paleomagnetic data from 5 dykes (6 sites) exhibit a dual-polarity magnetization with either west/up or east/down magnetizations (Fig. 9; Table 3d). The inverse baked contact test indicates that this magnetization is older than the SPG3-direction, and NW-shallow overprints indicate that it also predates 1765 Ma. The mean direction from these dykes falls at D= 261°, I= -51° (k= 37, α_{95}= 13°). Dykes have both northeast and northwest trends (Fig. 7).

5. Discussion

5.1 Magnetic Relationships within Singhbhum Craton

Paleomagnetic data from Neoarchean dykes were assumed to be primary in an earlier study by Kumar et al. (2017). This interpretation was based on several indirect arguments: that the magnetization is of dual-polarity, that the dual-polarities 'pass' a reversals test, and that no amphibolite-grade metamorphism has occurred in the craton post-dyke-emplacement (Kumar et al., 2017; Nelson et al., 2014).

There are issues with using these indirect arguments as proxies for direct evidence. First, directions acquired during a remagnetization event can be of dual-polarity (Johnson and Van der Voo, 1989). Second, the reversals test in any iteration (Merrill and McElhinny, 1990; Heslop and Roberts, 2018), merely tests for a common mean, not an emplacement time of the rock in question. Given the negative baked contact test described above, a positive reversals test does not preclude remagnetization. Third, although we agree that tectonothermal events in the Singhbhum probably failed to bring the cratonic interior above the blocking temperature of magnetite (Nelson et al., 2014; Kumar et al., 2017), replacement of a primary magnetic direction can take place at lower temperatures over extended periods (Pullaiah et al., 1975) or as the result of fluid flow (Geissman and Harlan, 2002).

A petrographic examination of the Neoarchean and Paleoproterozoic dykes (Kumar et al., 2017; Shankar et al., 2017), revealed hydrothermal alteration of both pyroxene and plagioclase (Sengupta et al., 2014). Low-temperature hydrothermal activity alters the primary magnetic signature of magnetite-bearing rocks (Ade Hall et al., 1971). Rock magnetic evidence from this study (e.g. demagnetization spectra and Curie temperature analysis) indicate that steep directions are isolated in magnetically-altered samples. Multiple post-Neoarchean intrusion events in Singhbhum Craton provide opportunities for thermal and/or hydrothermal alteration of the dykes and jointed, permeable dyke margins (Hall, 2008). Have these intrusive events also led to major changes in remanent paleomagnetic directions? The steep magnetization isolated along the fine-grained margins at sites I176, I1720, and I1734 indicate that remagnetization was over a period of at least one billion years following the emplacement of Neoarchean dykes. This steep

SPG2 direction is similar that isolated in Neoarchean dykes (Kumar et al., 2017). This is troubling to reconcile with a primary Neoarchean magnetization, but does not necessarily exclude the possibility given the long timescales involved (Pivarunas et al., 2018). Further, the confidence interval on these overprints are relatively large (Fig. 6), thus, we do not regard these data as conclusive evidence against a primary magnetization in the Neoarchean dykes. We note that SPG2 is primarily isolated as a high-temperature/coercivity component in NNE-trending dykes, as was noted by Kumar et al. (2017).

There are myriad episodes of Paleoproterozoic dyke emplacement within the craton (Shankar et al., 2017; Srivastava et al., 2019). We surmise that these pulses of activity may be related to the SPG1-4 groups although we cannot place rigid age constraints on each one of the directional groups (Fig. 7).

The northwest shallow-up magnetic direction is geographically widespread in the Singhbhum Craton both as a primary magnetization in the 1765 Ma Piplia dyke swarm and as dual-polarity overprint in older dykes (Shankar et al., 2017; Srivastava et al., 2019). The Piplia swarm dykes are also sometimes overprinted by two distinct secondary magnetizations – a steep secondary component, and a NE-shallow secondary component (Supplement). Therefore, the 1765 Ma direction serves as a magnetic time marker in the Singhbhum craton.

5.2 Comparison to the other South Indian cratons

The assembly of Peninsular India might be resolved with paleomagnetic data from its constituent cratons including data from the Singhbhum Craton. Since the Neoarchean dykes in Singhbhum Craton cannot be shown to preserve a primary magnetization, and similarly, no primary Neoarchean paleomagnetic data from either Dharwar or Bastar cratons exist, the very ancient comparative paleoposition of these cratons remains inscrutable to paleomagnetic analysis. In contrast, the Paleoproterozoic positioning of the Indian cratons is more amenable to paleomagnetic methods. There are multiple phases of Paleoproterozoic dyke emplacement in Singhbhum Craton, either absolutely or relatively dated (Shankar et al., 2014; Kumar et al., 2017; Srivastava et al., 2019), some of which reset the magnetic record of earlier dykes.

Thus, despite age uncertainty, we present the following comparisons of Singhbhum paleomagnetic data with Paleoproterozoic poles from the Dharwar and Bastar cratons (Table 4). The most well-supported comparison is between coeval 2250-2207 Ma dykes within both Singhbhum (Kaptipada dyke; Srivastava et al., 2019) and Dharwar (Kumar et al., 2015; Nagaraju et al., 2018a, b) cratons. The Kaptipada dyke has a NE-trend, as do other dykes in Singhbhum Craton, including many dykes within the SPG1-4 datasets.

The SPG1 pole falls near the 2250-2207 Ma swath of early Paleoproterozoic paleomagnetic poles from Dharwar Craton (at 2250 Ma, 2216 Ma, and 2207 Ma; Fig. 13a). The mean paleomagnetic pole for SPG1 dykes of Singhbhum Craton is 40° N, 105° E (A95=9.5°). The corresponding 2250 Ma paleomagnetic pole from the Dharwar Craton falls at 13° N, 116° E (A95=14°; Nagaraju et al., 2018b, as recalculated in Meert et al., in press). While the poles appear to be distinct, they can be aligned by a simple Euler rotation of the Singhbhum Craton centered in the Mahanadi Rift (21° N, 84° E, -60°). Figure 13b shows one possible reconstruction including the Dharwar-Bastar and Singhbhum cratons, both without rotation and with rotation. Thus, the SPG1 data may provide evidence for a loose amalgam of the South Indian Blocks in the Paleoproterozoic. However, in the absence of precise knowledge of the ‘magnetic’ age for the SPG1 paleomagnetic data, this is speculative. Paleomagnetic data from the precisely-dated Kaptipada dyke (2252 Ma) will provide critical information for this hypothesis.

The ages for SPG2, SPG3 and SPG4 remain a mystery; however, we suspect that at least some of the steeper directions isolated in SPG2 pre-date 1765 Ma, given that the characteristic directions in some of these groups are partially overprinted by 1765 Ma directions. Other than the 2250-2207 Ma poles cited above, there are additional poles that are older than 1765 Ma recorded in the Dharwar/Bastar cratons (Table 4). Of those, only the 2367 Ma inclinations are steep enough to be considered a possible match for SPG2. The SPG2 pole falls at 9.1° N, 78.3° E (A95=8.4°) and the grand mean 2367 Ma pole for the combined Dharwar-Bastar-SGT region falls at 13° N, 62° E (A95=5°). These two poles are different (non-overlapping A95 envelopes); however, applying the same Euler rotation given above, the two poles are brought into statistical alignment (Fig. 13a). We are tentative about such a correlation because at least some of the steep directions used to calculate SPG2 may be younger than 1765 Ma.

We make a final point of comparison with SPG4 and the 1888 Ma pole from Dharwar Craton (Belica et al., 2014). We suggest the Bhagamunda swarm, constrained in age between 2.26 Ga and 1.77 Ga (Srivastava et al., 2019) as a possible candidate for SPG4. The SPG4 virtual geomagnetic pole is at 18.2° N, 147.6° E (A95=15.6°). We use the same Euler rotation as with SPG1 and SPG2, and observe that SPG4 falls closer to the 1885 Ma Dharwar paleomagnetic pole after rotation (Fig. 13a). These comparisons, particularly those of SPG2 and SPG4, are preliminary. However, the repeatedly improved fits after applying the same Euler rotation to these Singhbhum data are intriguing.

A recent discovery of a 1794 Ma dyke in the Dharwar Craton might indicate broadly coeval activity in both the Singhbhum and Dharwar cratons (Söderlund et al., 2019); however, paleomagnetic data are lacking from the Dharwar dyke. The late Paleoproterozoic 1765 Ma Pipilia dyke swarm is, in contrast, the best-constrained paleomagnetic datum from Singhbhum craton. Comparison of this with Dharwar (and Bastar) Craton paleomagnetic data will be crucial moving forward.

A northeast-shallow-inclination paleomagnetic data from Singhbhum Craton overprints, and therefore post-dates, primary 1765 Ma data (Fig. 4; Supplementary Material). Given the distribution of dykes with comparable paleomagnetic data across the entire Singhbhum Craton, northeast-shallow-inclination direction are likely the result of a regional remagnetization event. Major orogenic activity north of Singhbhum Craton, in the Chhotanagpur Granite-Gneiss Complex, occurred at ~1.0-1.1 Ga (Bhowmik, 2019). If the northeast-shallow-inclination Singhbhum magnetization resulted from orogenic activity at this time, then it should be comparable with ca. 1.0 Ga paleomagnetic data from neighboring cratons. A paleomagnetic pole calculated from remanent magnetization with ~1.1 Ga Dharwar Craton kimberlites (Venkateshwarlu et al., 2013) falls at 45°N, 195°E (A95=15°) and a mean paleomagnetic pole from sedimentary and igneous rocks in the Bundelkhand Craton falls at 43°N, 216°E (A95=7°; Meert et al., 2021). These are comparable to the paleomagnetic pole calculated from Singhbhum dykes overprinted with northeast-shallow-inclination directions at 34°N, 196°E (A95=11°). Thus, these paleomagnetic data from Singhbhum Craton likely represent paleomagnetic disturbance from orogenic activity associated with North India Block – South India Block assembly.

5.3 Global Tectonic Implications

Previous paleogeographic models assumed that the Neoarchean dykes from the Singhbhum Craton record a primary magnetization. Based on that assumption, Kumar et al. (2017) and Chaudhuri (2020) speculated that the Singhbhum Craton was part of the supercraton "Vaalbara" (Cheney, 1996). Given the caveats noted above with respect to evidence for a primary magnetization, we believe these data are currently unsuitable for constraining spatial relationships within reconstructions of Vaalbara. Primary paleomagnetic data from the Paleoproterozoic likely survives within Singhbhum Craton. The key takeaway from the comparison of Paleoproterozoic paleomagnetism from Dharwar and Singhbhum Cratons is that the South Indian blocks were a loose amalgam during the Paleoproterozoic.

The 1765 Ma data from Singhbhum Craton are currently the best option for use in global reconstructions. Singhbhum Craton occupied equatorial latitudes (Fig. 14).

Several well-constrained paleomagnetic poles from other cratons are available from around 1765 Ma (±25 Myr) (Table 5). The most reliable paleomagnetic data from this interval were used to construct Figure 15. The 1.756 Ga Newer Dolerite NW-SE trending swarm (Table 1) places the South Indian Blocks. The Volyn-Dniestr-Bug Intrusions (Elming et al., 2010) are used for Sarmatia, while a combination of poles from ~1785 locates Fennoscandia (Pisarevsky and Sokolov, 2001; Elming et al., 2009; Elming et al., 1994; Mertanen et al., 2006). This separation is consistent with models positing the final rotation of Sarmatia into the Baltica assemblage from 1.72-1.66 Ga (Elming et al., 2010). Other poles used include: the 1.741 Ga Cleaver dykes-Laurentia (Irving et al., 2004); the 1.789 Ga Avanavero mafic rocks-Amazonia (Bispo-Santos et al., 2014); 1.769 Ga Taihang dykes-N. China (Halls et al., 2000; Xu et al., 2014), and the Elgety Formation-Siberia (Didenko et al., 2015). A dyke swarm in the Congo-Sao Francisco Craton (CSF) at 1790 Ma illustrates a 'bar-code' age match with both South India cratons and North China Craton (NCC); we incorporate its paleomagnetic data (Agrella-Filho et al., 2020) to place CSF into our reconstruction as well.

This late Paleoproterozoic configuration of continents positions Laurentia against the Baltica blocks along the Greenland-Fennoscandian margins (as in Evans and Mitchell (2011) and Zhang et al. (2012) among others) and Amazonia is placed equatorially, adjacent to both future Baltica and Siberia (Aldan). Assuming Dharwar-Bastar-Singhbhum contiguity at this time (Fig. 15), we place the southern Indian blocks together and adjacent to North China Craton, and relatively close to Siberia, and Amazonia. Thus, the majority of paleomagnetic data reveal their associated blocks were at lower latitudes, with the exception of Laurentia. The South Indian blocks have been linked with both Baltica (Pisarevsky et al., 2013; Pisarevsky et al., 2014), and North China (Zhao et al., 2002; Zhao et al., 2003; Clark et al., 2012; Zhang et al., 2012) in the Paleoproterozoic-Mesoproterozoic. Detrital zircon spectra used by Clark et al. (2012) on rocks from the Vestfold Hills (VH) in East Antarctica led to the proposal of a Neoarchean collision between NCC and SIB. This was a modification of an earlier proposal by Zhao et al. (2003) who linked NCC and the SIB on the basis of general similarities in their Archean to Paleoproterozoic basement sedimentary and magmatic successions. The 1765 Ma paleomagnetic pole from the Singhbhum Craton is supportive of these models. We argue it is now – and has been – untenable to link the Central Indian Tectonic Zone (CITZ) and Trans-North China Orogen (TNCO), based on more recent, detailed geochronological studies of both the orogens (e.g. TNCO: Zhang et al., 2006; CITZ: Bhowmik et al., 2012; Bhowmik et al., 2019). This is also supported by the inferred spatial orientation of the orogens as shown in Figure 15. Note, major tectonism along the CITZ post-dates our reconstruction by >150 Myr. Both ages and geometric considerations, therefore, mitigate against unity of the large central orogens of North China Craton and cratonic India central orogen unity. We also emphasize that Peninsular India as a united entity was not fully amalgamated at this time – since it came together along the Central Indian Tectonic Zone.

6. Conclusions

Our new results demonstrate that the Singhbhum Craton has a complex paleomagnetic history. With the pervasive thermal and hydrothermal alteration within Singhbhum Craton, all reported Precambrian paleomagnetic directions require rigorous field tests to ensure their stability and primary nature. Additionally, particularly for small dykes, the trends of dykes may not be reliably correlative with ages. Our data generally agrees with earlier findings (Shankar et al., 2017; Kumar et al., 2017).

The reported 1765 Ma paleopole for the Singhbhum Craton (Shankar et al., 2017) represents a primary magnetic signature. We provide additional data and calculated a new mean paleomagnetic pole for the Singhbhum Craton at 1765 Ma. Given the presence of a reverse polarity dyke within our new data, this pole now grades out at R=6 (Meert et al., 2020). The 1765 Ma magnetization is also prevalent as an overprint in older dykes throughout the craton. Thus, we can use the emplacement of this dyke swarm as a useful reference point for paleomagnetic studies within the craton.

Kumar et al. (2017) identified a steep, dual-polarity direction on NNE-trending Neoarchean mafic dykes of the Singhbhum Craton. Kumar et al. (2017) argued that the dual-polarity remanence provided evidence for a primary magnetization. Our detailed sampling, baked contact tests, and rock magnetic results provide complicated evidence for steep magnetizations, both predating and postdating 1765 Ma. Thus, there is equivocal support for the survival of a primary Neoarchean magnetization; however, we consider that a primary magnetic signal from the Neoarchean is not well supported by evidence. There are clear indications of magnetizations pre-dating and post-dating the 1765 Ma dykes.

We have identified these as SPG1-4 and provide the following summary regarding their relative ages. SPG1 compares favorably to mid-Paleoproterozoic data from the Dharwar Craton – a fellow piece of the present South Indian blocks. We propose that SPG1 paleomagnetic data is from the 2250 Ma Kaptipada dyke swarm. As such, this implies a loose configuration of Singhbhum, Dharwar, and Bastar cratons dating back to early within the Paleoproterozoic. The key test of this hypothesis is direct paleomagnetic examination of the Kaptipada dyke itself. SPG2 is an odd case, its paleomagnetic directions are similar to overprints on 1765 Ma dykes, which implies this paleomagnetic signature postdates 1765 Ma and is late Paleoproterozoic or Mesoproterozoic. Baked contact tests show similarity between these directions and the host rocks of the craton. However, other evidence, such as Neoarchean dyke ages, overprints of 1765 Ma age, and an unusually strong trend-paleomagnetic affinity for this group may imply certain directions of this age are older. SPG3 and SPG4 both are likely primary, Paleoproterozoic paleomagnetic data which pre-date 1765 Ma; SPG4 is the older of the two.

Thus, paleomagnetic data from Singhbhum Craton indicate that it is a rich trove of Paleoproterozoic paleomagnetic data. Refining these data and tightening the timing of South Indian Block assembly via comparison of Singhbhum and Dharwar paleomagnetism should be a future priority of Precambrian Indian paleomagnetic studies.

Acknowledgments

This work was primarily supported by the USA National Science Foundation grants **EAR13-47942 and EAR18-50693** to JGM. All conclusions of this paper are those of the authors and not the funding agency. AFP was supported by a Graduate Student Fellowship from the University of Florida. The Master's thesis work of KDK was instrumental in putting together the complex narrative of Singhbhum paleomagnetism. We also thank Rachel Nutter and Patrick Denning for work on sample analysis. We are grateful to the Ivar Giæver Geomagnetic Laboratory (IGGL) for the use of their facilities during a visit by AFP. The IGGL is funded by the Research Council of Norway (project #226214) and the Centre for Earth Evolution and Dynamics, University of Oslo. We appreciate the constructive and detailed attention of three reviewers, among them Elisa Piispa, whose reviews significantly improved this manuscript. The helpful editorial handling of Guest Editors Dey and Jayananda is appreciated.

Figure Captions

Figure 1. Cratonic sketch map of Peninsular India adapted from Meert et al., (in press) showing major Archean nuclei and tectonic features such as basins and mobile belts. Abbreviations as follows: **Basin Names**: MB=Marwar Basin; VB=Vindhyan Basin; ChB=Chhattisgarh Basin; CuB=Cuddapah Basin; KBB=Kaladgi-Bhima Basin; IB=Indravati Basin; PG=Prahnita-Godavari Basin; MR=Mahanadi Rift. **Tectonized Regions**: NSL=Narmada-Son Lineament; AFB=Aravalli Fold Belt; DFB=Delhi Fold Belt; CIS=Central Indian Suture; CITZ=Central Indian Tectonic Zone; SMB=Satpura Mobile Belt (~equivalent to CITZ); ; CGGC=Chotanagpur Granite Gneiss Complex; EGMB=Eastern Ghats Mobile Belt; PCSZ=Palghat-Cauvery Shear Zone; RP=Rengali Province; **Other Abbreviations**: CG=Closepet Granite; R=Rajmahal Traps; WDC=Western Dharwar Craton; EDC=Eastern Dharwar Craton; SIB=Southern Indian Blocks (the Dharwar, Bastar and Singhbhum cratons); NIB=Northern Indian Blocks (the Aravalli and Bundelkhand Cratons).

Figure 2. Simplified geological map (GSI 1:2M geology, 1998) of Singhbhum Craton and sampling sites, line segments indicating dyke trends as determined via field observations and satellite imagery. Radiometrically dated dykes are indicated by stars. Heavily sampled areas which lack detail on this scale are indicated as KR – Kanjhari Reservoir and BK – Bhima Kunda. They are detailed with finer-scale mapping in the Supplementary Material associated with this paper. BG = Bonai Granite. Other units as labeled, geology is approximate. Inset map to the top left indicates location of Singhbhum Craton within major provinces of peninsular India: SC: Singhbhum Craton, BC: Bastar Craton, DC: Dharwar Craton, SGT: Southern Granulite Terrain, DT: Deccan Traps, AC: Aravalli Craton, BuC: Bundelkhand Craton.

Figure 3: (a) Paleomagnetic data from Singhbhum Craton at 1765 Ma. (a) Directional results from this study (Table 2) are combined with extant data (Shankar et al., 2017) to calculate a revised mean direction. (b,c, e) Examples of demagnetization behavior (closed/open symbols represent declination/inclination in Zijderveld diagrams; closed/open symbols represent down/up inclinations in stereoplots, (d) Temperature-susceptibility curves for representative samples indicating magnetite with growth of new magnetic phases upon heating.

Figure 4: (a) Baked contact test on the large 1765 Ma dyke (I1637+I171) at its intersection with a smaller, older dyke (I172). The small dyke and some distance into the granite have been baked by the large dyke. (b,c) Zijderveld plots showing demagnetization behavior at the baked contact test. A secondary magnetization difficult to remove by thermal treatment alone has affected the large dyke post-emplacement. (d) An intensity decay curve (normalized to initial intensity) showing mixed thermal-AF treatment moving magnetization along great-circle trajectory northeast to northwest (e) Further stereonets of demagnetization data, principally from large WNW dyke (sites I1637 and I171)

illustrating examples of this overprint and the varied effects with different demagnetization options. Symbols are the same as in Figure 3.

Figure 5: An example of magnetic alteration along a dyke margin in Singhbhum Craton. (a) The stereoplot of directions recovered from a 1765 Ma WNW-trending dyke. (b) Zijderveld diagram of multi-component magnetization with a characteristic NW-shallow (primary) component. (c) sample from dyke margin with NNW-steep down magnetization isolated with thermal demagnetization (d) partner specimen demagnetized using AF reveals steep-down component unblocked at low coercivities and NW-shallow up characteristic direction isolated at higher coercivities along with (e) a stereoplot of the same sample. (e) A schematic location of samples. Symbols are the same as in Figure 3.

Figure 6. Magnetic overprints directions isolated from dyke samples includes (a) steep (dual polarity) and (b) NW-SE-shallow (dual polarity). Circles are individual site means; squares are means of all sites. These correspond with known data groupings such as SPG2 (Fig. 7, Section 4.2.2; although the confidence interval is quite large), and the 1765 Ma Singhbhum direction. Closed/open symbols represent down/up inclinations in stereoplots; Rose diagram indicates dyke trends.

Figure 7: Directional data from NNE-trending and WNW-trending dykes in Singhbhum Craton. Four distinct groups are recoverable, named here SPG1-4 (a-d), respectively corresponding to an interpreted 2250 Ma group, a group that corresponds with overprint directions (see Fig. 6), and two groups which each have nearly antipodal intermediate directions. Closed/open symbols represent down/up inclinations in stereoplots; Rose diagram indicates dyke trends. Color-group relationships carry into Figures 8 and 9.

Figure 8: Steep paleomagnetic data from Singhbhum Craton, with examples of different demagnetization behaviors shown from SPG1 (purple) and SPG2 (blue) dykes with Zijderveld plots and stereonets (symbols as in Fig. 3). Demagnetization behavior is quite variable (a) high-unblocking temperature direction (b) low-coercivity direction (c,d) NW-directed overprints on the steep component (e) temperature-susceptibility curves showing nearly reversible behavior (I1721) and alteration on heating of a low-temperature magnetic phase (I1726) (f) typical non-reversible temperature-susceptibility curves indicating growth of new magnetic phases during heating-cooling cycles.

Figure 9: Intermediate-inclination paleomagnetic data from Singhbhum Craton. Examples of different demagnetization behavior shown from SPG3 (orange) and SPG4 (green) dykes. (a) near univectorial thermal demagnetization sample (I1635-2a) and (b) substantial pyrrhotite carried overprint (I1730-A10a) (c) Temperature-susceptibility plots for selected samples for both groups. Behavior ranges from nearly reversible in some cases to more typical substantial growth of new magnetic phases during heating (d) SPG4 example yielding multicomponent behavior with a NW-down directed overprint. Symbols are the same as in Figure 3.

Figure 10: Baked contact tests for SPG1 at site I1427 (upper half) and SPG2 at site I178 (lower half). For SPG1 site I1427, (a) stereonet showing directional data (b,c) Zijderveld diagrams showing demagnetization behavior from dyke and host rocks, (d) schematic of baked contact test sampling (boxes indicate block sampling locations) and (e) bulk susceptibility profile. For SPG2 site I178, (f) directional data showing overlap in stereonet directional data (g) the sampling around the dyke (h,k) examples of Zijderveld plots of demagnetization behavior (i) bulk susceptibility profile (units in μSI), and j) susceptibility temperature experiment indicating the presence of pyrrhotite. Symbols as in Figure 3.

Figure 11: (a) Schematic illustration of cross-cutting dykes at Bhima Kunda section of the Baitarani River; (b) stereoplot of directions isolated from these dykes dashed lines represent low-temperature, low coercivity components color coded to the dykes. (c-f) Zijderveld diagrams and associated stereoplots showing directional behavior change in relationship to distance from dyke contact. Sample numbers are coded to labeled samples from (a) schematic. Symbols the same as in Figure 3. OP=overprint; CD=characteristic direction.

Figure 12. Baked contact test at site I1715. The (a) transects of samples across the dyke intersection, each circle indicating a separate core sample taken and the (b) stereonet of directions. Individual circles are individual sample overprint data, squares and triangles with confidence intervals are means of samples. Symbols same as in Figure 3. Far-field ChRMs refer to characteristic directions recovered from each separate dyke ~150 meters away from this outcrop. Cross-cutting relationships are not apparent at the physical outcrop.

Figure 13: (a) Comparison of paleomagnetic poles between Singhbhum and Dharwar cratons. Ages of Dharwar poles as indicated. Faded out Singhbhum poles are the in-situ positions, full-color represents the rotation of these poles (as given in Table 4). (b) Craton reconstructions for South Indian blocks throughout the Paleoproterozoic.

Figure 14: (a) Virtual geomagnetic poles (circles) from this work (Table 1) and overprints (Table 2a) Mean paleomagnetic poles – calculated as a mean of virtual geomagnetic poles (from ChRM directions of dykes) – shown with A95 confidence intervals. The small Singhbhum cratonic nucleus is shown within Singhbhum Craton. (b) Paleomagnetic reconstruction of India at 1765 Ma. Shaded out sections indicate modern positioning while bold colors indicate the reconstruction. India is placed at equatorial latitude and rotated with respect to present-day position.

Figure 15: Reconstruction from ca. 1770 Ma (adapted from Meert et al., in press) showing paleomagnetically permissible arrangement of cratonic blocks (rotation parameters are combination of reconstruction Euler poles and longitudinal rotations: Laurentia 0° N, 187° E, +71°; Fennoscandia 16.8° N, 140° E, +46.2°; Sarmatia 26.2° N, 26.6° E, -142.6°;Amazonia 67.8° N, 188° E, +142.7°; North China 25.7° N, 168.8° E, -+54.1°; Aldan 33° N, 128.5° E, +104.2°: South Indian Blocks 31° N, 245° E, +55.3°)The 'equatorial' blocks include Amazonia, the

South Indian blocks (Dharwar, Bastar, and Singhbhum), and North China TNCO=Trans North China Orogen (1.8-2.1 Ga).

References

Acharyya, S. K., Gupta, A., and Orihashi, Y., 2010. New U-Pb zircon ages from Paleo-Mesoarchean TTG gneisses of the Singhbhum Craton, eastern India. Geochemical Journal 44, 81-88.

Basu, A., Bickford, M. E., 2015. An alternate perspective on the opening and closing of the intracratonic Purana basins in peninsular India. Journal of the Geological Society of India 85, 5-25.

Belica, M.E., Piispa, E.J., Meert, J.E., Pesonen, L.J., Plado, J., Pandit, M.K., Kamenov, G.D., Celestino, M., 2014. Paleoproterozoic mafic dyke swarms from the Dharwar craton; paleomagnetic poles for India from 2.37 to 1.88 Ga and rethinking the Columbia supercontinent. Precambrian Research 244, 100–122.

Bhowmik, S.K., Chattopadhyay, A., Gupta, S., Dasgupta, S., 2012. Proterozoic tectonics: An Indian perspective on the Central Indian Tectonic Zone (CITZ). Proceedings of the Indian National Scientific Academy 78, 385-391.

Bhowmik, S. K., 2019. The current status of orogenesis in the Central Indian Tectonic Zone: A view from its Southern Margin. Geological Journal 54, 2912-2934.

Bleeker W, and Ernst R. 2006. Short-lived mantle generated magmatic events and their dyke swarms: The key unlocking Earth's paleogeographic record back to 2.6 Ga. In Dyke Swarms - Time Markers of Crustal Evolution. Edited by E. Hanski, S. Mertanen, T. Rämö, and J. Vuollo. Taylor and Francis/Balkema, London, pp. 3-26.

Bose, M.K., 2008. Petrology and geochemistry of Proterozoic 'Newer Dolerite' and associated ultramafics within Singhbhum granite pluton, eastern India. In Srivastava, R.K., Shivaji, Ch., and Chalapathi Rao, V. eds., Indian Dykes: Geochemistry, Geophysics and Geochronology: Narosa, New Delhi, 413-446.

Chaudhuri, T., Wan, Y., Mazumder, R., Ma, M., & Liu, D., 2018. Evidence of enriched, hadean mantle reservoir from 4.2-4.0 Ga zircon xenocrysts from Paleoarchean TTGs of the Singhbhum Craton, Eastern India. Scientific reports 8, 1-12.

Chaudhuri, T., 2020. A review of Hadean to Neoarchean crust generation in the Singhbhum Craton, India and possible connection with Pilbara Craton, Australia: The geochronological perspective. Earth-Science Reviews, 103085.

Cheney, E.S., 1996. Sequence stratigraphy and plate tectonic significance of the Transvaal succession of southern Africa and its equivalent in Western Australia. *Precambrian Research*, *79*, 3-24.

Chetty, T.R.K, 2014. Deep crustal shear zones in the Eastern Ghats Mobile Belt, India: Gondwana correlations, Journal of the Indian Geophysical Union 18, 19-56.

Clark, C., Collins, A.S., Timms, N.E., Kinny, P.D., Chetty, T.R.K., Santosh, M., 2009. SHRIMP U-Pb age constraints on magmatism and high-grade metamorphism in the Salem Block, Southern India. Gondwana Research 16, 27-36.

Clark, C., Kinny, P. D., Harley, S. L., 2012. Sedimentary provenance and age of metamorphism of the Vestfold Hills, East Antarctica: evidence for a piece of Chinese Antarctica?. Precambrian Research 196, 23-45.

Das, A.K., Piper, J.D.A, Mallik, S.B., and Sherwood, G.J., 1996. Paleomagnetic study of Archaean Banded Hematite Jasper Rocks from the Singhbhum-Orissa Craton, India. Precambrian Research 80, 193-204.

Dasgupta S., Bose S., Bhowmik S.K., Sengupta P., 2017. The Eastern Ghats Belt, India, in the context of supercontinent assembly. In: Dasgupta S, Pant NC (eds) Crustal evolution of India and Antarctica: the supercontinent connection, v. 457. Geological Society London Special Publications, London, pp 87–104.

Dasgupta, P., Ray, A., and Chakraborti, T. M., 2019. Geochemical characterisation of the Neoarchaean newer dolerite dykes of the Bahalda region, Singhbhum craton, Odisha, India: Implication for petrogenesis. Journal of Earth System Science 128, 216.

Dash, J.K., Pradhan, S.K., Bhutani, R., Balakrishnan, S., Chandrasekaran, G., Basavaiah, N., 2013. Paleomagnetism of ca. 2.3 Ga mafic dyke swarms in the northeastern Southern Granulite Terrain, India: Constraints on the position and extent of Dharwar craton in the Paleoproterozoic. Precambrian Research 228, 164-176.

Deenen, M. H., Langereis, C. G., van Hinsbergen, D. J., Biggin, A. J., 2014. Geomagnetic secular variation and the statistics of palaeomagnetic directions. Geophysical Journal International 186, 509-520.

Dey, S.; Topno, A.; Liu, Y.; and Zong, K. 2017. Generation and evolution of Palaeoarchaean continental crust in the central part of the Singhbhum craton, eastern India. Precambrian Research 298, 268–291.

Dey, S., Nayak, S. K., Mitra, A., Zong, K., and Liu, Y., 2020. Mechanism of Paleoarchean continental crust formation as archived in granitoids from the northern part of Singhbhum Craton, eastern India. Geological Society, London, Special Publications 489, 189-214.

Demirer, K., 2012. U–Pb Baddeleyite Ages from Mafic Dyke Swarms in Dharwar Craton, India –Links to an Ancient Supercontinent, (Dissertations in Geology at Lund University, Master’s thesis), 308 pp.

Didenko, A.N., Vodovozov, V.Yu., Peskov, A.Yu., Guryanov, V.A., Kosynkin, A.V., 2015. Paleomagnetism of the Ulkan massif (SE Siberian platform) and the apparent polar wander path for Siberia in late Paleoproterozoic–early Mesoproterozoic times. Precambrian Research, 259, 58-77.

Elming, S.A., 1994. Paleomagnetism of Precambrian rocks in northern Sweden and its correlation to radiometric data, Precambrian Research, 69, 61-79.

Elming, S. Å., Moakhar, M. O., Layer, P., Donadini, F., 2009. Uplift deduced from remanent magnetization of a proterozoic basic dyke and the baked country rock in the Hoting area, Central Sweden: a palaeomagnetic and 40Ar/39Ar study. Geophysical Journal International 179, 59-78.

Elming, S. Å., Shumlyanskyy, L., Kravchenko, S., Layer, P., Söderlund, U., 2010. Proterozoic Basic dykes in the Ukrainian Shield: A palaeomagnetic, geochronologic and geochemical study—The accretion of the Ukrainian Shield to Fennoscandia. Precambrian Research 178, 119-135.

Evans, D.A.D., Mitchell, R.N., 2011. Assembly and breakup of the core of Paleoproterozoic–Mesoproterozoic supercontinent Nuna. Geology 39, 443–446.

Everitt, C.W.F., Clegg, J.A., 1962. A field test of palaeomagnetic stability. Geophysical Journal International 6, 312–319.

Fisher, R. A., 1953. Dispersion on a sphere. Proceedings of the Royal Society of London. Series A. Mathematical and Physical Sciences 217, 295-305.

French, J.E., Heaman, L.M., Chacko, T., Srivastava, R.K., 2008. 1891-1883 a southern Bastar craton-Cuddapah mafic igneous events, India: a newly recognized large igneous province. Precambrian Research 160, 308–322.

French, J.E., Heaman, L.M., 2010. Precise U-Pb dating of Paleoproterozoic mafic dyke swarms of the Dharwar craton, India: implications for the existence the Neoarchean supercraton Sclavia. Precambrian Research 183, 416-441.

Geissman, J.W., Harlan, S.H., 2002. Late Paleozoic remagnetization of Precambrian crystalline rocks along the Precambrian/Carboniferous nonconformity, Rocky Mountains: a relationship among deformation, remagnetization, and fluid migration. Earth and Planetary Science Letters 203, 905-924.

.

Gregory, L. C., Meert, J. G., Pradhan, V., Pandit, M. K., Tamrat, E., Malone, S. J., 2006. A paleomagnetic and geochronologic study of the Majhgawan kimberlite, India: Implications for the age of the Upper Vindhyan Supergroup. Precambrian Research 149, 65–75. https://doi.org/10.1016/j.precamres.2006.05.005.

GSI 1:2M Map, 1998. Geological Survey of India, 1:2M Geological Map. Accessed through Bhukosh Portal, 2019.

Halls, H.C., Li, J.-H., Davis, D., Hou, G.-T., Zhang, B.-X., Qian, X.-L., 2000. A precisely dated Proterozoic paleomagnetic pole from the North China craton, and its relevance to paleocontinental reconstruction. Geophysical Journal International 143, 185–203.

Halls, H.C., Kumar, A., Srinivasan, R., Hamilton, M.A., 2007. Paleomagnetism and U–Pb geochronology of easterly trending dykes in the Dharwar craton, India: feldspar clouding, radiating dyke swarms and the position of India at 2.37 Ga. Precambrian Research 155, 47–68.

Halls, H.C., 2008. The importance of integrating paleomagnetic studies of Proterozoic dykes with U-Pb geochronology and geochemistry. In: Srivastava, R.K., Sivaji, Ch., Chalapathi Rao, N.V. (eds), Indian Dykes: Geochemistry, Geophysics, and Geochronology, Naroosa Publishing, New Delhi, 19-40.

He, Y.-H., Zhao, G.-C., Sun, M., Xia, X.-P., 2009. SHRIMP and LA-ICP-MS zircon geochronology of the Xiong'er volcanic rocks: implications for the Paleo-Mesoproterozoic evolution of the southern margin of the North China Craton. Precambrian Research 168, 213–222.

Heslop, D., Roberts, A.P., 2018. Revisiting the paleomagnetic reversal test: A Bayesian hypothesis testing framework for a common mean direction, Journal of Geophysical Research: Solid Earth 123, 7225-7236.

Jain, A.K., Banerjee, D.M. and Kale, V.S., 2020. Tectonics of the Indian subcontinent. Journal of Earth System Science, 129, 224. https://doi.org/10.1007/s12040-020-01501-1

Jayananda, M., Dey, S., and Aadhiseshan, K. R., 2020). Evolving early earth: Insights from peninsular India. Geodynamics of the Indian Plate, 5-103.Johnson, R. J., & Van der Voo, R., 1989. Pre-folding magnetization reconfirmed for the Late Ordovician-Early Silurian Dunn Point volcanics, Nova Scotia. Tectonophysics 178, 193-205.

Katusin, K.D., 2017. Paleomagnetism of Proterozoic Newer Dolerites Dyke in the Singhbhum Craton, NE India, (University of Florida, Master's thesis), 81 pp.

Kirschvink, J.L., 1980. The least squares line and plane and the analysis of paleomagnetic data. Geophysical Journal of the Royal Astronomical Society 62, 699–718.

Kumar, A., Bhalla, M.S., 1984. Palaeomagnetism of Sukinda chromites and their geological implications. Geophysical Journal 77, 863-874.

Kumar, A., Parashuramulu, V., Nagaraju, E., 2015. A 2082 Ma radiating dyke swarm in the Eastern Dharwar Craton, southern India and its implications to Cuddapah basin formation. Precambrian Research 288, 490-505.

Kumar, A., Parashuramulu, V., Shankar, R., Besse, J., 2017. Evidence for a Neoarchean LIP in the Singhbhum craton, eastern India: Implications to Vaalbara supercontinent. Precambrian Research 292, 163-174.

Liao, A.C-Y., Shellnutt, J.G., Hari, K.R., Denyszyn, S.W., Vishwakarma, N., Verma, C.B., 2019. A petrogenetic relationship between bonititic dyke swarms of the Indian shield: Evidence from the central Bastar Craton and the NE Dharwar craton, Gondwana Research 69, 193-211.

Mahadevan, T.M., 2002. Geology of Bihar and Jharkhand. Geological Society of India, Bangalore. 563 pp.

Malone, S.J., Meert, J.G., Banerjee, D.M., Pandit, M.K., Tamrat, E., Kamenov, G.D., Pradhan, V.R., Sohl, L.E., 2008. Paleomagnetism and detrital zircon geochronology of the Upper Vindhyan sequence, Son Valley and Rajasthan, India: A ca. 1000 Ma closure age for the Purana basins? Precambrian Research 164, 137-159.

McFadden, P.L., McElhinney, M.W., 1990. Classification of the reversal test in paleomagnetism. Geophysical Journal International 103, 725–729.

Meert, J. G., Pandit, M. K., 2015. The Archaean and Proterozoic history of Peninsular India: tectonic framework for Precambrian sedimentary basins in India. Geological Society of London Memoirs 43, 29-54.

Meert, J.G., Pandit, M.K., Pradhan, V.R., Banks, J.C., Sirianni, R., Stroud, M., Newstead, B., Gifford, J., 2010. The Precambrian tectonic evolution of India: A 3.0-billion-year odyssey. Journal of Asian Earth Sciences 39, 483-515.

Meert, J.G., Pandit, M.K., Pradhan, V.R., Kamenov, G.D., 2011. Preliminary report on the paleomagnetism of 1.88 Ga dykes from the Bastar and Dharwar cratons, Gondwana Research 20, 335-343.

Meert, J.G., Pivarunas, A.F., Miller, S.R., Nutter, R.F., Pandit, M.K., Sinha, A.K, 2021 The Precambrian drift history and paleogeography of India, in: Pesonen et al.(eds) Precambrian Paleomagnetism and Supercontinents, Elsevier, in press.

Meert, J. G., Pivarunas, A. F., Evans, D. A., Pisarevsky, S. A., Pesonen, L. J., Li, Z. X., ... & Salminen, J. M., 2020. The magnificent seven: A proposal for modest revision of the quality index. Tectonophysics 790.

Meißner, B., Deters, P., Srikantappa, C., Köhler, H., 2002. Geochronological evolution of the Moyar, Bhavani and Palghat shear zones of southern India: implications for east Gondwana correlations. Precambrian Research 114, 149-175.

Mertanen, S., Eklund, O., Shebanov, A., Frank-Kamenetsky, D., Vasilieva, T., 2006a. Palaeo- and Mesoproterozoic dyke swarms in the Lake Ladoga area, NW Russia - Palaeomagnetic studies. In: Hanski, E., Mertanen, S., Rämö, T., Vuollo, J. (eds.) Dyke Swarms - Time Markers of Crustal Evolution. Taylor & Francis, London, pp. 63–74.

Miller, K. C., and Hargraves, R. B., 1994. Paleomagnetism of some Indian kimberlites and lamproites. Precambrian Research 69, 259-267.

Miller, S.R., Mueller, P.A., Meert, J.G., Kamenov, G.D., Pivarunas, A.F., Sinha, A.K., Pandit, M.K. 2018. Detrital zircons reveal evidence of Hadean crust in the Singhbhum craton, India, Journal of Geology.

Mir, A.R., Shabber, H.A., and Balaram, V., 2011. Geochemistry, petrogenesis and tectonic significance of the Newer Dolerites from the Singhbhum Orissa craton, eastern Indian shield. International Geology Review 53, 46-60.

Mir, A.R. and Alvi, S.H., Geochemistry of Ultramafic Dykes from Chaibasa District, Singhbhum craton, Eastern India: Petrogenetic and Tectonic Implications.

Misra, S., Johnson, P. T., 2005. Geochronological constraints on evolution of Singhbhum mobile belt and associated basic volcanics of eastern Indian shield. Gondwana Research 8, 129-142.

Mukherjee, S., Dey, A., Sanyal, S., Ibanez-Mejia, M., Dutta, U., Sengupta, P., 2017. Petrology and U–Pb geochronology of zircon in a suite of charnockitic gneisses from parts of the Chotanagpur Granite Gneiss Complex (CGGC): evidence for the reworking of a Mesoproterozoic basement during the formation of the Rodinia supercontinent. Geological Society, London, Special Publications 457, 197-231.

Mukhopadhyay, J., Beukes, N. J., Armstrong, R. A., Zimmermann, U., Ghosh, G., Medda, R. A., 2008. Dating the oldest greenstone in India: a 3.51-Ga precise U-Pb SHRIMP zircon age for dacitic lava of the southern Iron Ore Group, Singhbhum craton. The Journal of Geology 116, 449-461.

Mukhopadhyay, J., Crowley, Q.G., Ghosh, S., Ghosh, G., Chakrabarti, K., Misra, B., Heron, K. and Bose, S., 2014. Oxygenation of the Archean atmosphere: New paleosol constraints from eastern India. Geology 42, 923-926.

Naqvi, S.M., Rogers, J.J.W., 1987. Precambrian Geology of India. Oxford University Press, Oxford, pp. 223.

Nelson, D.R., Bhattacharya, H.N., Thern, E.R., Altermann, W., 2014. Geochemical and ion-microprobe U-Pb zircon constraints on the Archaean evolution of Singhbhum Craton, eastern India. Precambrian Research 255, 412–432.

Nagaraju, E., Parashuramulu, V., Ramesh Babu, N., & Narayana, A. C., 2018a. A 2207 Ma radiating mafic dyke swarm from eastern Dharwar craton, Southern India: Drift history through Paleoproterozoic. Precambrian Research, 317, 89–100. https://doi.org/10.1016/j.precamres.2018.08.009

Nagaraju, E., Parashuramulu, V., Anil Kumar, & Srinivas Sarma, D., 2018b. Paleomagnetism and geochronological studies on a 450 km long 2216 Ma dyke from the Dharwar craton, southern India. Physics of the Earth and Planetary Interiors, 274(, 222–231. https://doi.org/10.1016/j.pepi.2017.11.006

Peng, P., Zhai, M.-G., Zhang, H.-F., Guo, J.-H., 2005. Geochronological constraints on the Paleoproterozoic evolution of the North China craton: SHRIMP zircon ages of different types of Mafic dikes. International Geological Reviews 47, 492–508.

Piper, J.D.A., Zhang, J.-S., Huang, B.-C., Roberts, A.P., 2011. Paleomagnetism of Precambrian Dyke Swarms in the North China Shield: The 1.8 Ga LIP event and crustal consolidation in late Paleoproterozoic times. Journal of Asian Earth Sciences 41, 504–524.

Pisarevsky, S.A., Sokolov, S.J., 2001. The magnetostratigraphy and a 1780 Ma paleomagnetic pole from the red sandstones of the Vazhinka River section, Karelia, Russia. Geophysical Journal International, 146, 531-538.

Pisarevsky S., A., Biswal, T.K., Xuan-Ce Wang, B.C., De Waele, B.E., Ernst, R., Ulf Söderlund, U.H., Tait, J.A., Ratre, K., Singh, Y.K., Cleve, Mads, 2013. Palaeomagnetic, geochronological, and geochemical study of Mesoproterozoic Lakhna Dykes in the Bastar Craton, India: implications for the Mesoproterozoic supercontinent. Lithosphere 174, 125-143.

Pisarevsky, S.A., Elming, S.Å., Pesonen, L.J., Li, Z.X., 2014. Mesoproterozoic paleogeography: supercontinent and beyond. Precambrian Research 244, 207-225.

Pivarunas, A. F., Meert, J. G., Pandit, M. K., Sinha, A., 2019. Paleomagnetism and geochronology of mafic dykes from the Southern Granulite Terrane, India: Expanding the Dharwar craton southward. Tectonophysics 760, 4-22.

Pradhan, V.R., Meert, J.G., Pandit, M.K., Kamenov, G., Gregory, L.C., Malone, S.J., 2010. India's changing place in global Proterozoic reconstructions: New geochronologic constraints on key paleomagnetic poles from the Dharwar and Aravalli/Bundelkhand cratons. Journal of Geodynamics 50, 224–242.

Pradhan, V.R., Meery, J.G., Pandit, M.K., Kamenov, G., and Mondal, Md. E.A., 2012. Paleomagnetic and geochronological studies of the mafic dyke swarms of Bundelkhand craton, central India: Implications for the tectonic evolution and paleogeographic reconstructions. Precambrian Research 198-199, 51-79.

Pullaiah, G.E., Irving, E., Buchan, K.L., Dunlop, D.J., 1975. Magnetization changes caused by burial and uplift. Earth and Planetary Science Letters 28, 133-143.

Radhakrishna, T., Krishnendu, N., Balasubramonian, G., 2013. Palaeoproterozoic Indian shield in the global continental assembly: evidence from the palaeomagnetism of mafic dyke swarms. Earth Science Reviews 126, 370–389.

Rajesham, T, Bhaskar Rao, Y.J., Murti, K.S., 1993. The Karimnagar granulite terrain – a new sapphirine-bearing granulite province, South India. Journal of the Geological Society of India 41, 51-59.

Ramakrishnan, M., and Vaidyanadhan, R., 2008. *Geology of India*. Bangalore, Geological Society of India, 552 pp.

Samal, A.K., Srivastava, R., Sinha, L.K., 2015. ArcGIS studies and field relationships of Paleoproterozoic mafic dyke swarms from the south of Devarakonda area, eastern Dharwar craton, southern India: implications for their relative ages, Journal of Earth Systems Science 124, 1075-1084.

Santosh, M., Yokoyama, K., & Acharyya, S. K. 2004. Geochronology and tectonic evolution of Karimnagar and Bhopalpatnam Granulite Belts, Central India. *Gondwana Research*, *7*(2), 501–518. https://doi.org/10.1016/S1342-937X(05)70801-7

Shankar, R., Vijayagopal, B., Kumar, A., 2014. Precise Pb–Pb baddeleyite ages of 1765 Ma for a Singhbhum 'newer dolerite' dyke swarm. Current Science 106, 1306–1310.

Shankar, R., Sarma, D. S., Babu, N. R., Parashuramulu, V., 2017. Paleomagnetic study of 1765 Ma dyke swarm from the Singhbhum Craton: Implications to the paleogeography of India. Journal of Asian Earth Sciences.

Sengupta, P., Arijit Ray, A., Pramanik, S., 2014. Mineralogical and chemical characteristics of newer dolerite dyke around Keonjhar, Orissa: Implication for hydrothermal activity in subduction zone setting. Journal of Earth System Science 123, 887–904.

Sharma, R.S., 2009. Cratons and Fold Belts of India. Springer Verlag, Heidelberg, 324 pp.

Shellnutt, J. G., Hari, K. R., Liao, A. C. Y., Denyszyn, S. W., Vishwakarma, N., 2018. A 1.88 Ga giant radiating mafic dyke swarm across southern India and Western Australia. Precambrian Research 308, 58-74.

Singh, A. K., Upadhyay, D., Pruseth, K. L., Mezger, K., Nanda, J. K., Maiti, S., and Saha, D., 2021. Shock Metamorphic Features in the Archean Simlipal Complex, Singhbhum Craton, Eastern India: Possible Remnant of a Large Impact Structure. Journal of the Geological Society of India 97, 35-47.Söderlund, U., Bleeker, W., Demirer, K., Srivastava, R. K., Hamilton, M., Nilsson, M., Srinivas, M., 2019. Emplacement ages of Paleoproterozoic mafic dyke swarms in eastern Dharwar craton, India: Implications for paleoreconstructions and support for a∼ 30° change in dyke trends from south to north. Precambrian Research 329, 26-43.

Sreenivas, B., Dey, S., Rao, Y.B., Kumar, T.V., Babu, E.V.S.S.K. and Williams, I.S., 2019. A new cache of Eoarchaean detrital zircons from the Singhbhum craton, eastern India and constraints on early Earth geodynamics. Geoscience Frontiers 10, 1359-1370.

Srivastava, R.K., Ellam, R.M. and Gautam, G.C., 2009. Sr–Nd isotope geochemistry of the early Precambrian sub-alkaline mafic igneous rocks from the southern Bastar craton, Central India. Mineralogy and Petrology 96, 71-79.

Srivastava, R.K., Söderlund, U., Ernst, R.E., Mondal, S.K., Samal, A.K., 2019. Precambrian mafic dyke swarms in the Singhbhum craton (eastern India) and their links with dyke swarms of the eastern Dharwar craton (southern India), Precambrian Research 329, 5-17.

Srivastava, R.K., Singh, R.K., Verma, R., 2000. Juxtaposition of India and Antarctica During the Precambrian: Inferences from Geochemistry of Mafic Dykes. Gondwana Research, v.3, p. 227-234.

Tauxe, L. Shaar, R., Jonestrask, L., Swanson-Hysell, N.L., Minnett, R., Koppers, A.A.P., Constable, G.C., Jarboe, N., Gaastra, K. Fairchild, L. 2016. PmagPy: Software package for paleomagnetic data analysis and a bridge to the Magnetics Information Consortium (MagIC) Database, Geochemistry, Geophysics Geosystems 17**,** doi:10.1002/2016GC006307.

Torsvik, T.H., Doubrovine, P., Domeier, M., 2016. IAPD 2016. Center for Earth Evolution and Dynamics.

Upadhyay, D., Chattopadhyay, S. and Mezger, K., 2019. Formation of Paleoarchean-Mesoarchean Na-rich (TTG) and K-rich granitoid crust of the Singhbhum craton, eastern India: Constraints from major and trace element geochemistry and Sr-Nd-Hf isotope composition. Precambrian Research 327, 255-272.

Van der Voo, R., 1990. The reliability of paleomagnetic data. Tectonophysics 184, 1-9.

Venkateshwarlu, M., & Chalapathi Rao, N. V., 2013. New palaeomagnetic and rock magnetic results on Mesoproterozoic kimberlites from the Eastern Dharwar craton, southern India: Towards constraining India's position in Rodinia. Precambrian Research 224, 588–596. https://doi.org/10.1016/j.precamres.2012.11.003

Verma, R.K., Prasad, S.N., 1974. Paleomagnetic Study and Chemistry of Newer Dolerites from Singhbhum, Bihar, India. Canadian Journal of Earth Sciences 11, 1043-1054.

Wang, Y.-J., Fan, W.-M., Zhang, Y.-H., Guo, F., Zhang, H.-F., Peng, T.-P., 2004. Geochem-ical,40Ar/39Ar geochronological and Sr–Nd isotopic constraints on the origin of Paleoproterozoic mafic dikes from the southern Taihang Mountains and implications for the ca. 1800 Ma event of the North China Craton. Precambrian Research 135, 55–77.

Xu, H., Yeng, Z., Peng, P., Meert, J.G., Zhu, R., 2014. Paleoposition of the North China craton within the supercontinent Columbia: constraints from new Paleoproterozoic paleomagnetic results, Precambrian Research 255, 276-293.

Zhang, S.-H., Li, Z.-X., Evans, D.A.D., Wu, H.-C., Li, H.-Y., Dong, J., 2012. Pre-Rodinia supercontinent Nuna shaping up: A global synthesis with new paleomagnetic results from North China. Earth and Planetary Science Letters 353, 145–155.

Zhang J., Zhao G., Sun M., Wilde S.A., Li S., Liu S. 2006. High-pressure mafic granulites in the Trans-North China Orogen: tectonic significance and age. Gondwana Research 9, 349–362, https://doi.org/10.1016/j.gr.2005.10.005

Zhao, G.-C., Cawood, P.A., Wilde, S.A., Sun, M., 2002. Review of global 2.1–1.8Ga orogens: implications for a pre-Rodinia supercontinent. Earth-Science Reviews 59, 125–162.

Zhao, G.-C., Sun, M., Wilde, S.A., 2003. Correlations between the eastern block of the North China craton and the south Indian block of the Indian Shield: an Archaean to Paleoproterozoic link. Precambrian Research 122, 201–233.

Tables

Tables are placed here to use the landscape page orientation so as not to cut off data.

Table 1: 1765 Ma paleomagnetic results from Singhbhum Craton

Site	Lat (°N)	Lon (°E)	Trend (°)	N/n	Dec (°)	Inc (°)	a95 (°)	k	VGP Lat (°N)	VGP Lon (°E)
I144	22.6137	86.1000	130	9/8	284.4°	-16.5°	12.2°	21.5	9.8°	342.6°
I145	22.6077	86.0790	130	13/11	133.9°	-18.1°	12.5°	14.3	43.9°	347°
I147	22.6317	86.0607	20	7/3	342°	-18.1°	GC	GC	53.5°	296.9°
1765+[1]	21.5932	85.7263	120	5/59/48	327.4°	-17.4°	11.4°	65.8	45.8°	315.5°
I176+[2]	21.5983	85.7460	130	2/23/16	323.4°	-9.9°	42.0°	37.4	45.4°	323.5°
I1720+[3]	21.5177	85.9115	100	2/23/20	333.4°	-18.9°	12.7°	388.5	49.3°	308.5°
I1723	21.8068	85.8436	20	14/8	295.1°	-9.3°	15.0°	14.6	21.2°	341.4°
I1729	21.3513	85.9962	15	25/16	329.0°	5.0°	GC	GC	54.4°	328.2°
I1734+[4]	21.3727	86.1479	120	2/19/15	345.4°	-28.8°	15.8°	250.4	50.6°	288.6°
K11	21.59324	85.74369	122	10/10	332.5°	-35.1°	7.0°	56.0	41.0°	301.0°
K1	21.55161	86.01773	111	10/10	308.3°	-21.8°	2.0°	482.0	29.6°	328.2°
K15	21.43021	86.18127	118	8/8	326.5°	-22.4°	5.0°	129.0	43.4°	314.2°
K30	21.59685	85.88517	123	10/10	343.4°	-21.0°	6.0°	65.0	53.7°	294.2°
Mean Result				13 sites; N=230 n=183	321.6°	-15.7°	A95=12.9°	K=17.2	43.2°	319.9°

Notes: Site = name of cooling unit, +indicates multiple sites combined for a mean direction, ([1] = I1637, I171, I172, I1722, K10, SKJ10; [2] = I176+K12; [3] = I1720+K18; [4] = I1734+K14), italics are reported data from Shankar et al. (2017).. SLat = site latitude, SLon = site longitude, Trend = trend of dyke, N/n = total number of samples analyzed/number of samples suitable for analysis (a third number here reflects if multiple sites were taken at the same cooling unit, Dec = paleomagnetic declination, Inc = paleomagnetic inclination, a95/A95 = cone of 95% confidence about the mean direction/mean of virtual geomagnetic poles, k/K = kappa precision parameter (Fisher, 1953) for mean of directions/virtual geomagnetic poles, VGP Lat = virtual geomagnetic pole latitude, VGP Lon = virtual geomagnetic pole longitude (these last two calculated from directional data and site location). GC=great circle analysis used to determine mean direction.

Table 2: Consistent paleomagnetic overprint directions from Singhbhum dykes

Site	Lat (°N)	Lon (°E)	Trend (°)	n	Component	Dec (°)	Inc (°)	a95 (°)	k
2a: Overprints from ~1765 Ma									
I148	22.6317	86.0600	130	8	LT-pyrr	314°	-12°	8.4°	45
I1411	22.4053	86.1475	150	9	LC	164.9°	15°	8.6°	36
I1418	22.6193	85.9807	40	6	LT	353°	-3°	11.8°	33
I1433	21.6428	85.6507	5	5	LT	345°	10.1°	21.9°	13
I1442	21.8317	85.8612	20	4	LT-pyrr	318°	28.6°	18.6°	28.6
I1429	21.4039	85.7399	24	9	LT	155°	4.1°	8°	43
I1636	21.5921	85.7251	10	10	LT	317.2°	22.8°	13.3°	14.1
I1643	21.5514	86.0173	140	15	LT/MT/HC	304.2°	-2.8°	24.7°	3.4
I1646	21.5534	86.0178	140	7	LT/MC	331.3°	-29.4°	13.8°	20
I1647+[1]	21.5534	86.0178	40	4	LT	317.6°	-37°	19.2°	42
I174	21.5944	85.7292	10	10	HC/LT	338.8°	-27.5°	24.3°	10
I177	21.6842	85.854	21	4	LT/LC	309.9°	-9°	7.8°	138
Mean				12/87		327.5°	-6.8°	14.1°	10.4
2b: Overprints on dykes of ~1765 Ma age									
I176	21.5983	85.746	130	11	LC/HT	212.1°	79.7°	9.5°	24.3
I1720	21.5177	85.9115	100	3	LC/HT	95.4°	72.3°	10.2°	147.5
I1729	21.3513	85.9962	15	7	LC/MT	128.1°	-70°	4.3°	447.6
I1734	21.3727	86.1479	120	4	LC/HT	17.1°	86.2°	4°	227.7
2c: Overprints consistent with present day field									
I1427	21.5506	85.6618	140	8	LT	10.1°	50.2°	11.6°	23.6
I1645	21.5516	86.0184	20	6	LT	358.8°	11.2°	11.9°	32.9
I1650	21.5205	86.0171	125	8	LT	13.8°	27.5°	17.8°	10.6
I1718	21.5733	21.5733	21	12	LT	5.5°	42.4°	16°	8.3
I1727	21.3514	21.3514	21	11	LT	358. 6°	33.3°	3.8°	142.1

I1732	21.3878	21.3878	21	13	LT	359.3°	41.2°	4.7°	77.3

Notes: Site = name of cooling unit, +indicates multiple sites combined for a mean direction, italics are reported data from Shankar et al. (2017), SLat = site latitude, SLon = site longitude, Trend = trend of dyke, N/n = total number of samples analyzed/number of samples suitable for analysis (a third number here reflects if multiple sites were taken at the same cooling unit, Dec = paleomagnetic declination, Inc = paleomagnetic inclination, a95 = cone of 95% confidence about the mean direction, k = kappa precision parameter (Fisher, 1953)

Table 3: Steep-intermediate inclination paleomagnetic results from Singhbhum Craton dykes of NNE (Neoarchean) and WNW trends

Site	Lat (°N)	Lon (°E)	Trend (°)	N/n	Component	Dec (°)	Inc (°)	a95/MAD (°)	k	Plat (°N)	VGP Lat (°N)	VGP Lon (°E)
3a: Singhbhum Paleomagnetic Group 1												
I148*	22.6317	86.06	130	11/6	GC	75.3°	71.7°	10.2°	GC	56.5°	26.8°	122.8°
I149	22.6214	86.0049	10	7/7	HT/HC	21.7°	72.9°	5.7°	114.7	58.4°	51.0°	103.9°
I1427	21.5506	85.6618	140	14/13	HT/HC	65.9°	78°	8.1°	27.3	67.0°	29.1°	109.8°
I1429*	21.4039	85.7399	24	11/9	HT/HC	67.9°	65.6°	3.9°	178.3	47.8°	30.4°	131.9°
I1432	21.31675	85.81697	165	6/5	HT	332°	76°	11.8°	43	63.5°	43.8°	68.9°
I1441	22.2062	86.1811	25	7/3	HC	207°	-82°	25°	26	-74.3°	-35.9°	274.9°
I1445	22.53	85.8657	40	7/5	GC	28°	76°	25.9°	GC	63.5°	45.0°	103.1°
I1450	22.423	86.078	40	10/10	HT/HC	228.3°	-67°	5.9°	67.1	-49.7°	-43.5°	307.9°
I1639	21.5656	85.7053	30	5/5	HT/HC	172.4°	-66.6°	6.1°	156.3	-49.1°	-61.8°	255.2°
I1641+[1]	21.5526	86.0172	120	2/17/16	HT/HC	74.3°	65.9°	4.6°	64.2	48.2°	26.2°	131.7°
I1645	21.5516	86.0184	20	6/6	HT	348°	80°	5.1°	175	70.6°	40.5°	80.8°
I1646+[2]*	21.5534	86.0178	140	2/13/9	HT/HC	59.5°	68.7°	6.8°	68	52.1°	35.4°	126.6°
I1647+[3]*	21.5534	86.0178	40	2/23/11	HT/HC	342.4°	75.7°	7.9°	34.1	63.0°	46.9°	74.4°
I1650	21.5205	86.0171	125	8/8	HT/HC	73.7°	74.2°	2.3°	589.1	60.5°	26.6°	117.9°
I173	21.5944	85.7282	10	11/11	HT/HC	142.1°	-70.9°	5.8°	63.7	-55.3°	-46.1°	235.5°
I174*	21.5944	85.7292	10	15/7	HT	77°	75°	7.4°	67	61.8°	25.0°	116.3°
I1718	21.5733	85.9943	175	13/6	HT/HC	151.2°	-78°	5.7°	138.8	-67.0°	-41.1°	251.5°
I1726	21.3532	85.9929	30	19/13	HT	10.3°	73.2°	2.8°	221.5	58.9°	51.8°	94.6°
I1733+[4]	22.5584	85.892	20	2/28/16	HT/HC	100.1°	66.6°	4.6°	64.5	49.1°	10.6°	126.8°

Mean-Downward				B=19		51.5°	+76.4°	5.7°	49.4			
Mean-Upward				B=5		179.9°	-75.6	11.9°	42.3			
Mean				B=24, n=166		218°	-77.3°	5.3°	41	65.3°	40.2°	104.6°
3b: Singhbhum Paleomagnetic Group 2												
I1424	21.5131	85.8614	30	11/8	HT/HC	284.8°	72.5°	4.9°	128.9	57.8°	25.9°	50.9°
I1426	21.5676	85.651	140	9/9	HT	228.8°	68.3	7.7°	45.8	51.5°	-5.4°	57.6°
I1636*	21.5921	85.7251	10	10/7	HT	326.6°	-81.3	12.6°	23.8	-73.0°	-7.2°	275.1°
I1649	21.5539	86.0175	20	7/7	LT/HT	140.8°	84.1	6.1°	98.3	78.3°	12.4°	93.5°
I1651	22.3823	86.0863	40	8/6	HT	230.1°	78.2	6.9°	95.2	67.3°	7.0°	68.7°
I177+[5]*	21.6842	85.854	17	2/22/20	HT/HC	11.7°	-67	8.8°	806	-49.7°	17.9°	257.9°
I178	21.6829	85.8548	10	13/11	HT/HC	192.1°	67°	9.2°	25.6	49.7°	-17.8°	77.7°
I1713+[6]	21.6645	85.8742	15	2/28/15	GC	103.6°	-68.2°	GC	GC	-51.3°	-25.1°	223.8°
I1721	21.5983	85.8927	10	13/13	HT/HC	324.5°	-77.8°	4.4°	90.3	-66.6°	-2.1°	279.2°
I1724	21.3678	85.98	20	14/14	HT/HC	203.9°	70.8°	2.6°	228.9	55.1°	-10.8°	72.3°
I1725	21.3643	85.986	50	16/15	HT/HC	91.9°	86.2°	2.2°	299.3	82.4°	20.9°	94.1°
I1728	21.3513	85.9956	0	7/7	HT/HC	132.2°	80.8°	4.6°	169.9	72.1°	8.8°	99.4°
I1732	21.3878	85.9041	30	15/14	HT	156.5°	70.3°	2.6°	242.6	54.4°	-11.6°	99.6°
Mean-Downward				B=9		204.6°	+81.7°	4.6°	53.8			
Mean-Upward				B=4		33.0°	-82.2°	15.0°	26.8			
Our Mean				B=13		202°	+80°	7°	36			
Grand Mean				B=24, n=233		206.2°	+81.8°	4.3°	47.5	73.9°	7.9°	79.3°
3c: Singhbhum Paleomagnetic Group 3												
BKBig+[7]*	21.5519	86.0174	120	4/33/23	HT/HC	101.3°	-46°	5.3°	33.3	-27.4°	-19.3°	198.7°
I1635	21.5891	85.7286	10	7/5	HT	74.5°	-38.5°	6.5°	137.8	-21.7°	5.4°	201.6°
I1442*	21.8317	85.8612	20	6/5	HT	112.6°	-45.1°	4.8°	252.9	-26.6°	-29.1°	195.1°

I1437	21.5526	86.0172	55	8/8	HT	55.9°	-51°	2.6°	454.8	-31.7°	14.5°	219.3°
I1452	22.6135	86.1838	40	10/8	HT	99.5°	-43.4°	11.9°	22.5	-25.3°	-17.6°	196.9°
I1730*	21.3516	86.0132	0	10/5	HT/HC	273°	57°	6.2°	151	37.6°	15.1°	31.0°
Mean				B=6, n=87		89.9°	-48.4°	12.8°	28.4	-29.4°	-10.4°	203.9°
3d: Singhbhum Paleomagnetic Group 4												
I1413	22.4053	86.1475	40	10/8	LT/LC	109.1°	58.1°	4.6°	148	38.8°	0.2°	133.6°
I1441	22.2062	86.1811	25	7/5	HT	240.6°	-45.3°	10.7°	52.5	-26.8°	-35.2°	338.2°
I1451	22.4112	86.0751	130	10/10	HT/HC	84.3°	59.8°	4.9°	98.9	40.7°	18.5°	138.8°
I1727	21.3514	85.9952	10	12/11	HT	258.1°	-42.4°	6°	58.4	-24.5°	-19.0°	336.3°
I1643+[8]*	21.5514	86.0173	140	2/21/4	HT	261.2°	-45.2°	13.7°	45.6	-26.7°	-17.0°	333.4°
Mean				B=5, n=56		261.0°	-51.1°	12.7°	36.75	-31.7°	-18.2°	327.6°

Notes: Site = name of cooling unit, +indicates data from multiple sites combined in mean ([1] sites I1438+I1641, [2] I1646+I1440, [3] sites I1647+I1439+I1717, [4] I1733+I1417, [5] I177+K7, [6] I1713+K9, [7] I1642+I1644+I1435+I1714+I1715, [8] I1643+I1436), asterisk indicates that site has an overprint consistent with 1765 Ma directions (see Fig. 8). 1. SLat = site latitude, SLon = site longitude, Trend = trend of dyke, N/n = total number of samples analyzed/number of samples suitable for analysis (a third number here reflects if multiple sites were taken at the same cooling unit), Component = demagnetization that best isolated mean component from site specimens (HC = high coercivity, HT = high temperature, MT = medium temperature, LT = low temperature, LC = low coercivity), Dec = paleomagnetic declination, Inc = paleomagnetic inclination, a95 = cone of 95% confidence about the mean direction, k = kappa precision parameter (Fisher, 1953), VGP Lat = virtual geomagnetic pole latitude, VGP Lon = virtual geomagnetic pole longitude (these last two calculated from directional data and site location). GC=great circle analysis used to determine mean direction.

Table 4: Poles from SPG1-4 as well as Paleoproterozoic poles from Dharwar Craton for comparison.

Names	**Craton**	**Plat (°N)**	**Plon (°N)**	**R. Plat (°N)**	**R. Plon (°E)**	**A95 (°)**	**Age**	**Reference**
SPG1	Singhbhum	40.2°	104.6°	15.4°	110.8°	9.5°	2250 Ma?	this study
SPG2	Singhbhum	07.9°	079.2°	18.0°	69.6°	8.4°	2765 Ma?	this study; Kumar et al., 2017
SPG3	Singhbhum	10.4°	023.9°	60.8°	21.4°	16°	unknown	this study
SPG4	Singhbhum	18.2°	147.6°	-26.2°	121.5°	15.6°	unknown	this study
2367 Ma	Dharwar	12.8°	062.0°	-	-	4.6°	2367 Ma	Belica et al., 2014
2250 Ma	Dharwar	12.8°	116.0°	-	-	14°	2250 Ma	Nagaraju et al., 2018a
2216 Ma	Dharwar	33.5°	124.0°	-	-	6.6°	2216 Ma	Nagaraju et al., 2018b
2207 Ma	Dharwar	51.2°	108.0°	-	-	9.2°	2207 Ma	Nagaraju et al., 2018a
2082 Ma	Dharwar	40.8	184.0°	-	-	4.6°	2082 Ma	Kumar et al., 2015
1888 Ma	Dharwar	34.0°	334.0°	-	-	4.5°	1885 Ma	Belica et al., 2014

Euler pole used to rotate SPG1-4 is (21°N, 84°E, -60°).

Table 5: Selected poles from other cratons for comparison with the Singhbhum Craton at ~1770 Ma

Names	**Terrane**	**Plat**	**Plon**	**A95**	**Age**	**Reference**
Volyn-Dniestr-Bug intrusions	Sarmatia	27°	169°	4°	1755 Ma	Elming et al., 2010
Mean-Hoting, Shoksa, Lake Ladoga, Kallax	Fennoscandia	46°	223°	10°	1785 Ma	Elming et al., 2009
Cleaver Dykes	Laurentia	19°	277°	6°	1741 Ma	Irving et al., 2004
Avanavero mafic rocks	Amazonia	-48°	28°	9°	1789 Ma	Bispos-Santos et al., 2014
Para de Minas dykes	Congo-Sao Francisco	-40°	197°	17°	1790 Ma	Agrella-Filho et al., 2020
Elgety Formation	Siberia	7°	184°	12.8°	1732	Didenko et al., 2015
Taihang dykes	North China	41°	246°	4°	1769 Ma	Halls et al., 2000; Xu et al., 2014
Newer Dolerites 1765 Ma group	South India	43°	320°	11°	1765 Ma	this study

Figures

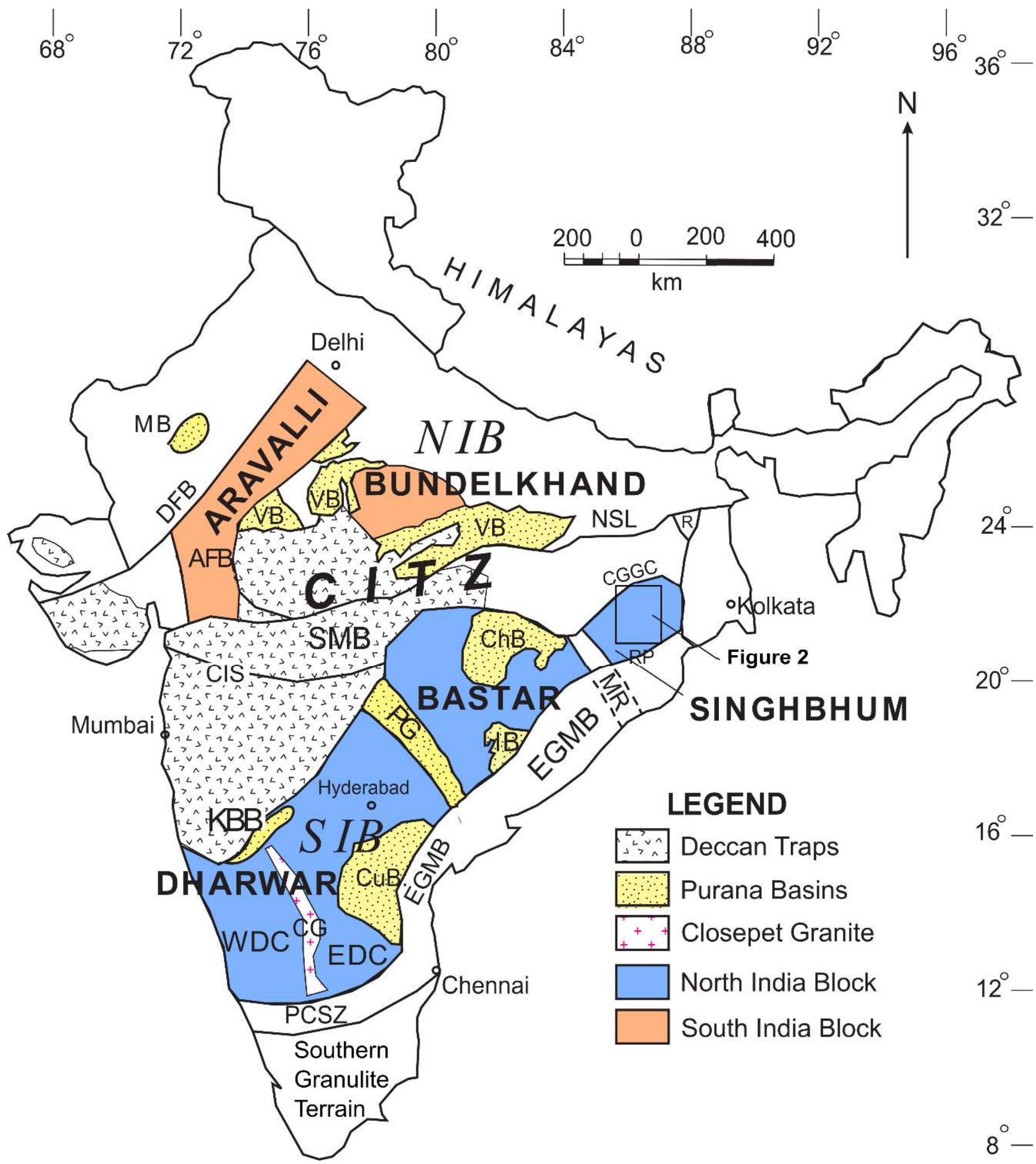
68°
72°
76°
80°
84°
88°
92°
96°
36°
32°
24°
20°
16°
12°
8°
N
200 0 200 400
km
HIMALAYAS
Delhi
MB
ARAVALLI
NIB
BUNDELKHAND
DFB
VB
VB
VB
NSL
R
AFB
CITZ
CGGC
Kolkata
SMB
ChB
Figure 2
RP
CIS
BASTAR
MR
SINGHBHUM
Mumbai
PG
IB
EGMB
Hyderabad
LEGEND
KBB
SIB
Deccan Traps
Purana Basins
DHARWAR
CuB
EGMB
Closepet Granite
CG
WDC
EDC
North India Block
Chennai
South India Block
PCSZ
Southern
Granulite
Terrain

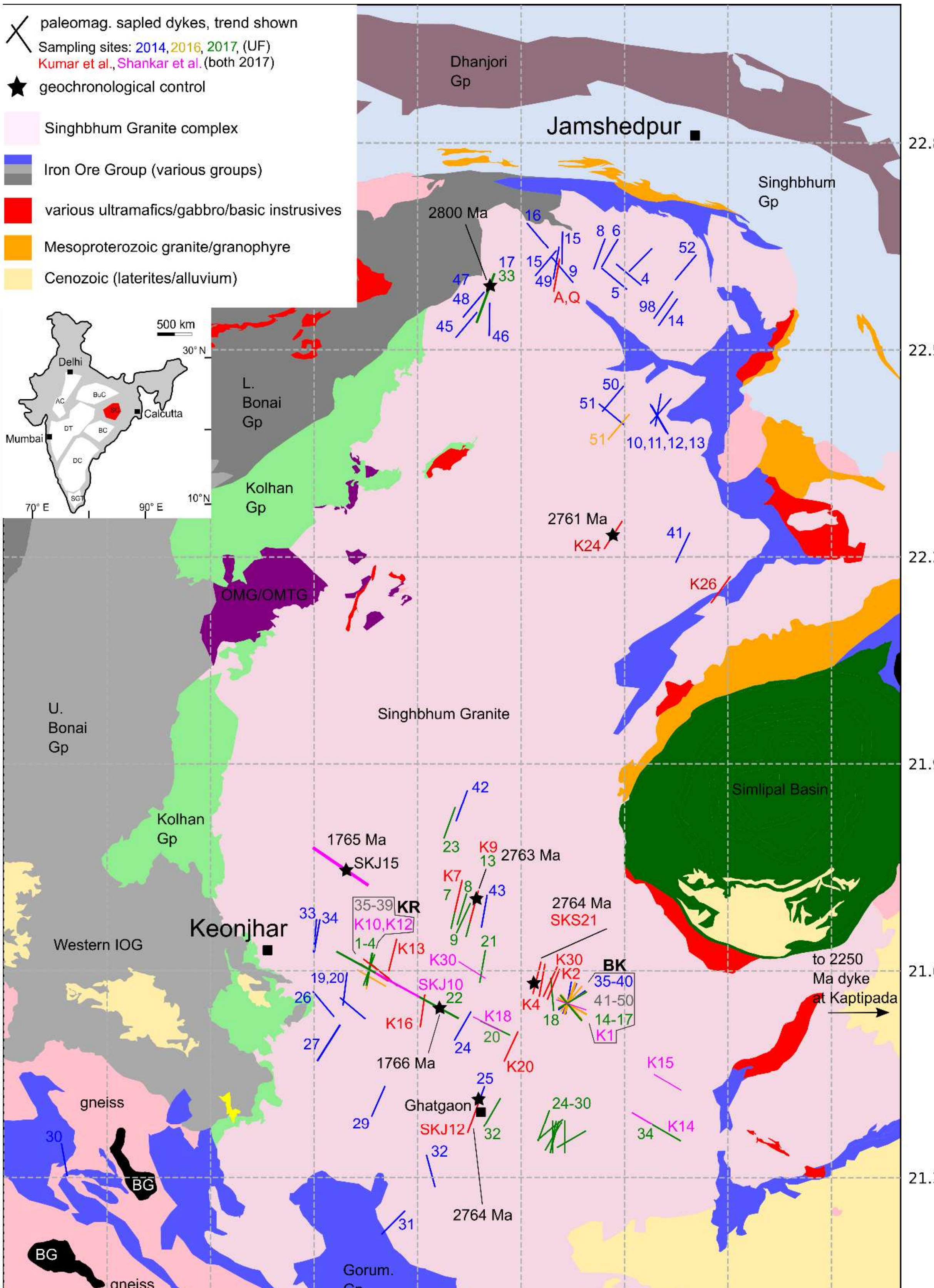

paleomag. sapled dykes, trend shown
Sampling sites: 2014, 2016, 2017, (UF)
Kumar et al., Shankar et al. (both 2017)
geochronological control
Singhbhum Granite complex
Iron Ore Group (various groups)
various ultramafics/gabbro/basic instrusives
Mesoproterozoic granite/granophyre
Cenozoic (laterites/alluvium)
500 km
Delhi
Calcutta
Mumbai
30° N
10° N
70° E
90° E
Dhanjori Gp
Jamshedpur
Singhbhum Gp
L. Bonai Gp
Kolhan Gp
OMG/OMTG
U. Bonai Gp
Singhbhum Granite
Simlipal Basin
Keonjhar
Western IOG
gneiss
BG
Gorum. Gp.
Ghatgaon
2800 Ma
2761 Ma
1765 Ma
SKJ15
2763 Ma
2764 Ma
SKS21
1766 Ma
KR
BK
to 2250 Ma dyke at Kaptipada
35-39
K10,K12
1-4
SKJ10
SKJ12
35-40
41-50
14-17
K1
K2
K4
K30
K24
K26
A,Q
85.35
85.50
85.65
85.80
85.95
86.10
86.25
86.40
22.8
22.5
22.2
21.9
21.6
21.3

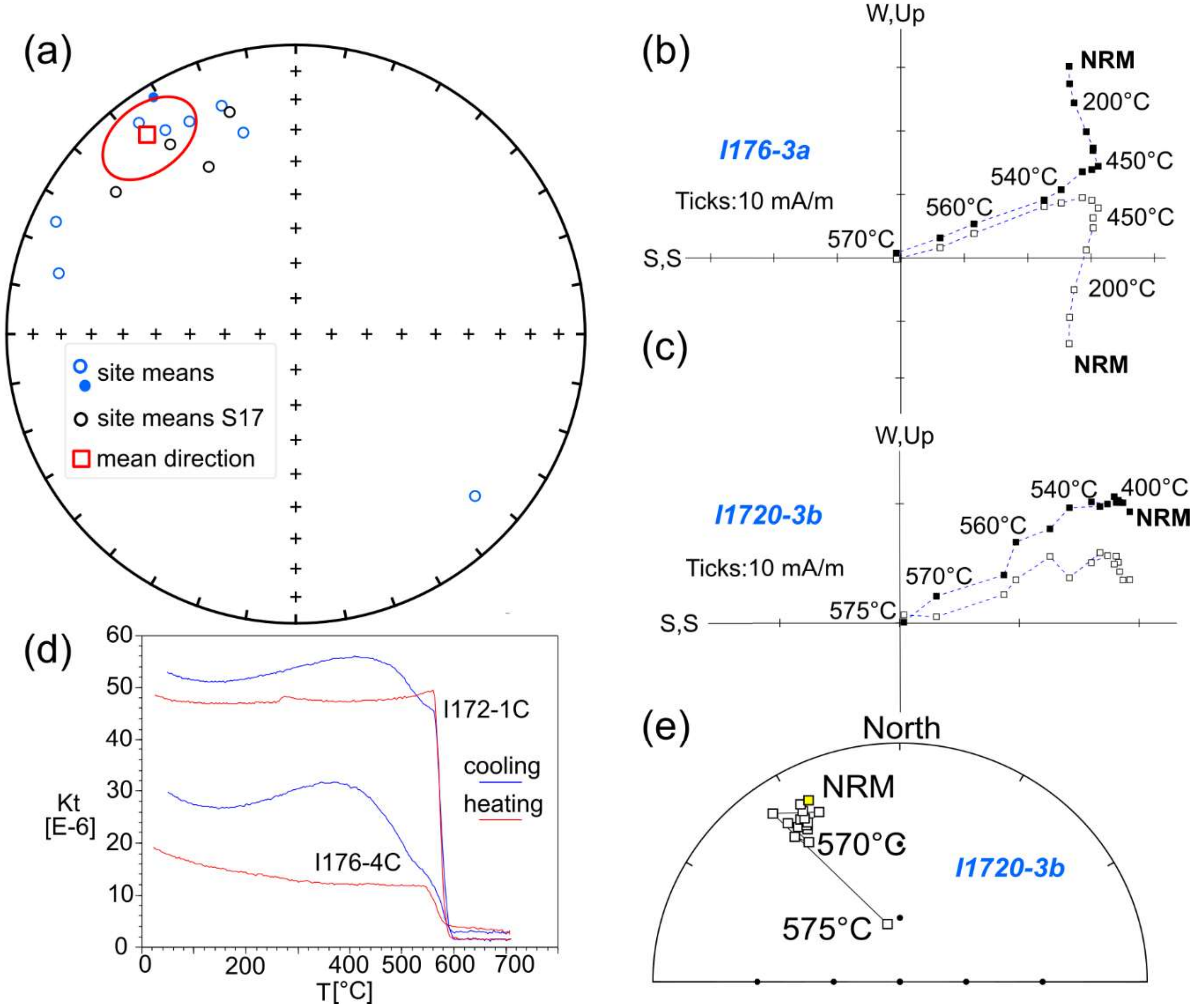

(a)
site means
site means S17
mean direction
(b)
W,Up
NRM
200°C
I176-3a
450°C
540°C
Ticks:10 mA/m
560°C
450°C
570°C
S,S
200°C
(c)
NRM
W,Up
540°C
400°C
I1720-3b
NRM
560°C
Ticks:10 mA/m
570°C
575°C
S,S
(d)
Kt
[E-6]
I172-1C
cooling
heating
I176-4C
T[°C]
(e)
North
NRM
570°C
I1720-3b
575°C

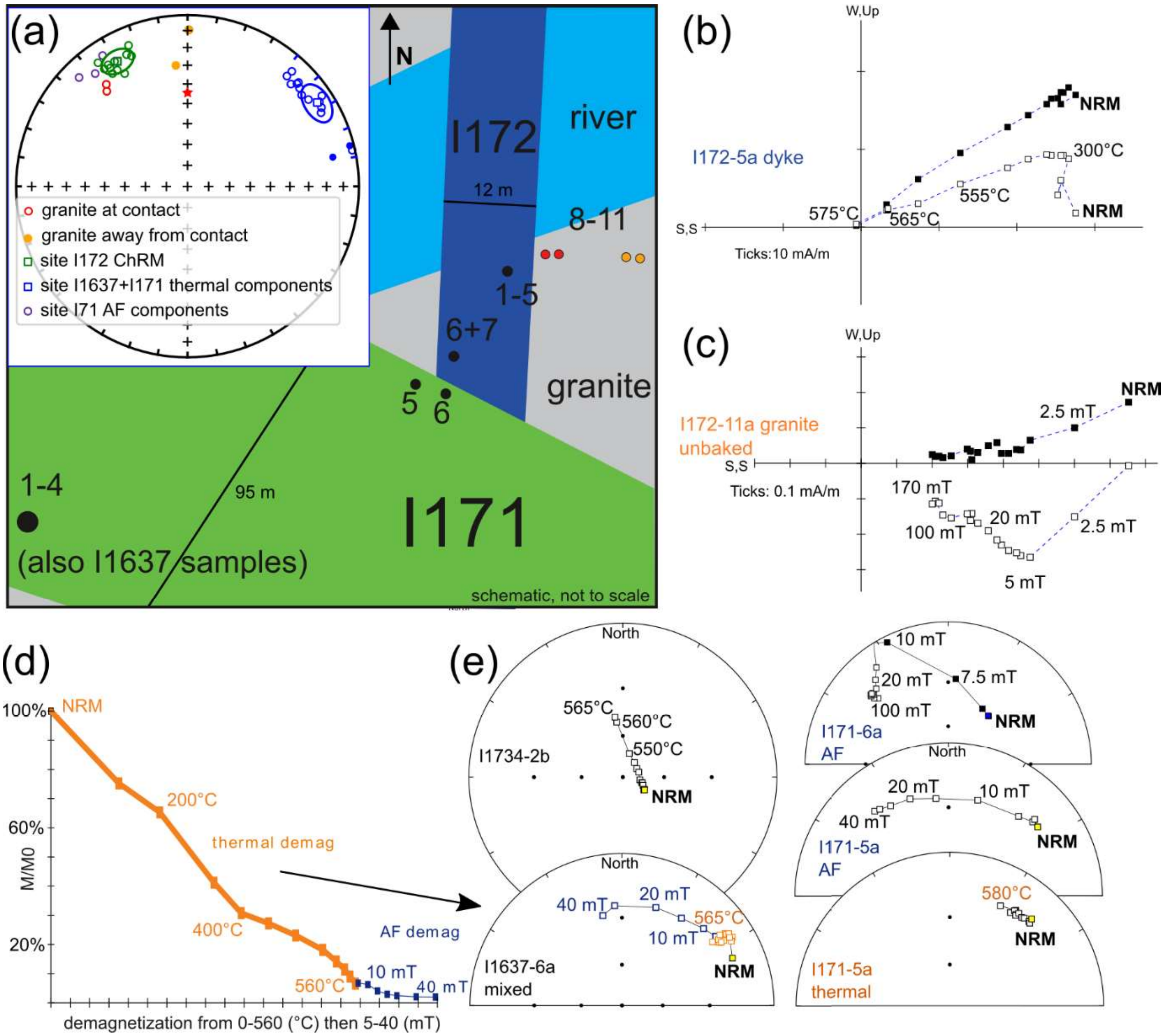

(a)
N
I172
river
12 m
8-11
1-5
6+7
granite
5
6
1-4
95 m
I171
(also I1637 samples)
schematic, not to scale
granite at contact
granite away from contact
site I172 ChRM
site I1637+I171 thermal components
site I71 AF components
(b)
W,Up
NRM
I172-5a dyke
300°C
555°C
575°C
565°C
S,S
Ticks:10 mA/m
(c)
W,Up
NRM
2.5 mT
I172-11a granite unbaked
S,S
Ticks: 0.1 mA/m
170 mT
100 mT
20 mT
2.5 mT
5 mT
(d)
100%
60%
20%
M/M0
NRM
200°C
thermal demag
400°C
AF demag
560°C
10 mT
40 mT
demagnetization from 0-560 (°C) then 5-40 (mT)
(e)
North
565°C
560°C
550°C
I1734-2b
NRM
I1637-6a mixed
40 mT
20 mT
10 mT
565°C
10 mT
7.5 mT
20 mT
100 mT
I171-6a AF
I171-5a AF
580°C
I171-5a thermal

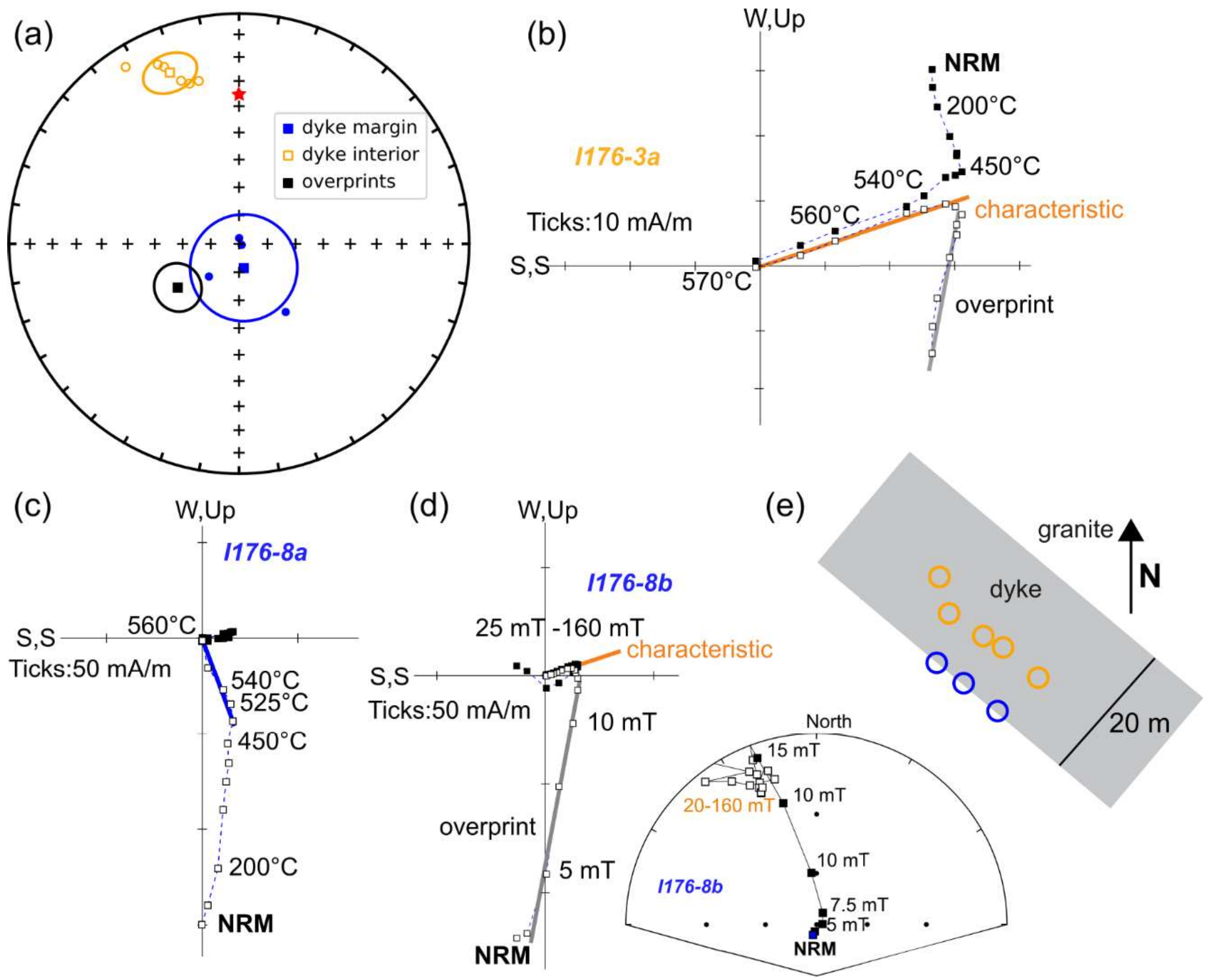

(a)
dyke margin
dyke interior
overprints
(b)
W,Up
NRM
200°C
I176-3a
450°C
540°C
560°C
characteristic
Ticks:10 mA/m
S,S
570°C
overprint
(c)
W,Up
I176-8a
560°C
S,S
Ticks:50 mA/m
540°C
525°C
450°C
200°C
NRM
(d)
W,Up
I176-8b
25 mT -160 mT
characteristic
S,S
Ticks:50 mA/m
10 mT
overprint
5 mT
NRM
North
15 mT
20-160 mT
10 mT
10 mT
I176-8b
7.5 mT
5 mT
NRM
(e)
granite
N
dyke
20 m

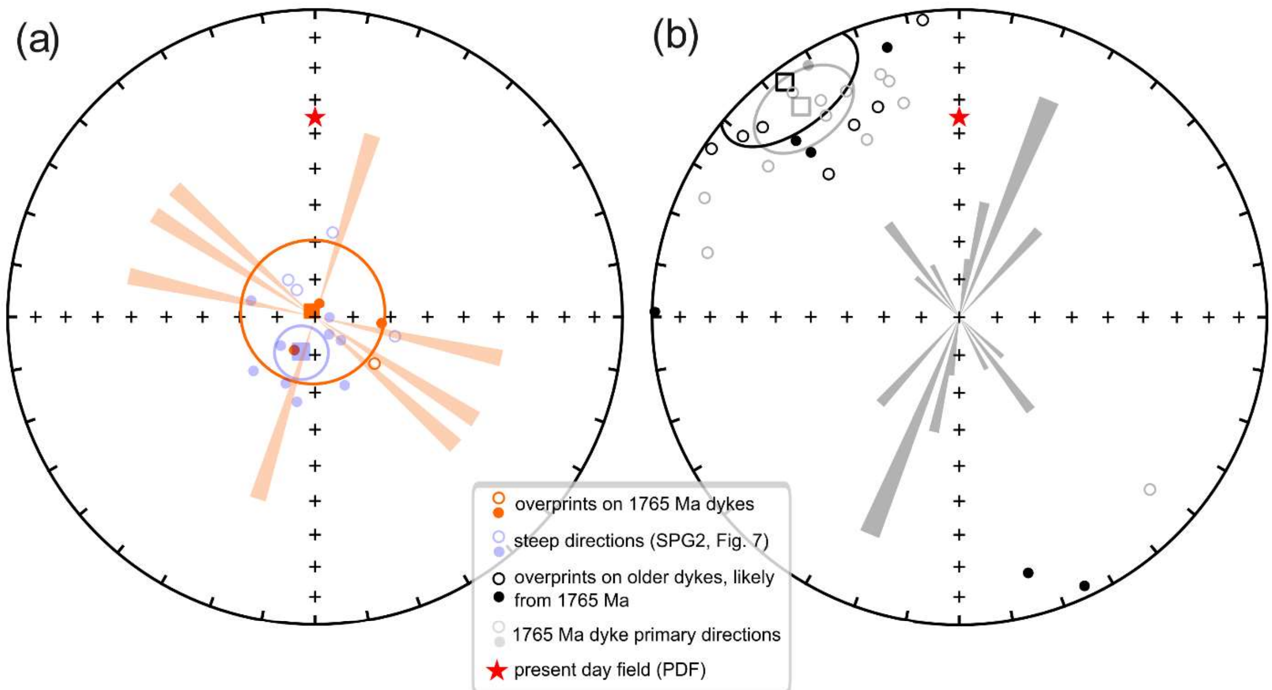
(a)
(b)
overprints on 1765 Ma dykes
steep directions (SPG2, Fig. 7)
overprints on older dykes, likely from 1765 Ma
1765 Ma dyke primary directions
present day field (PDF)

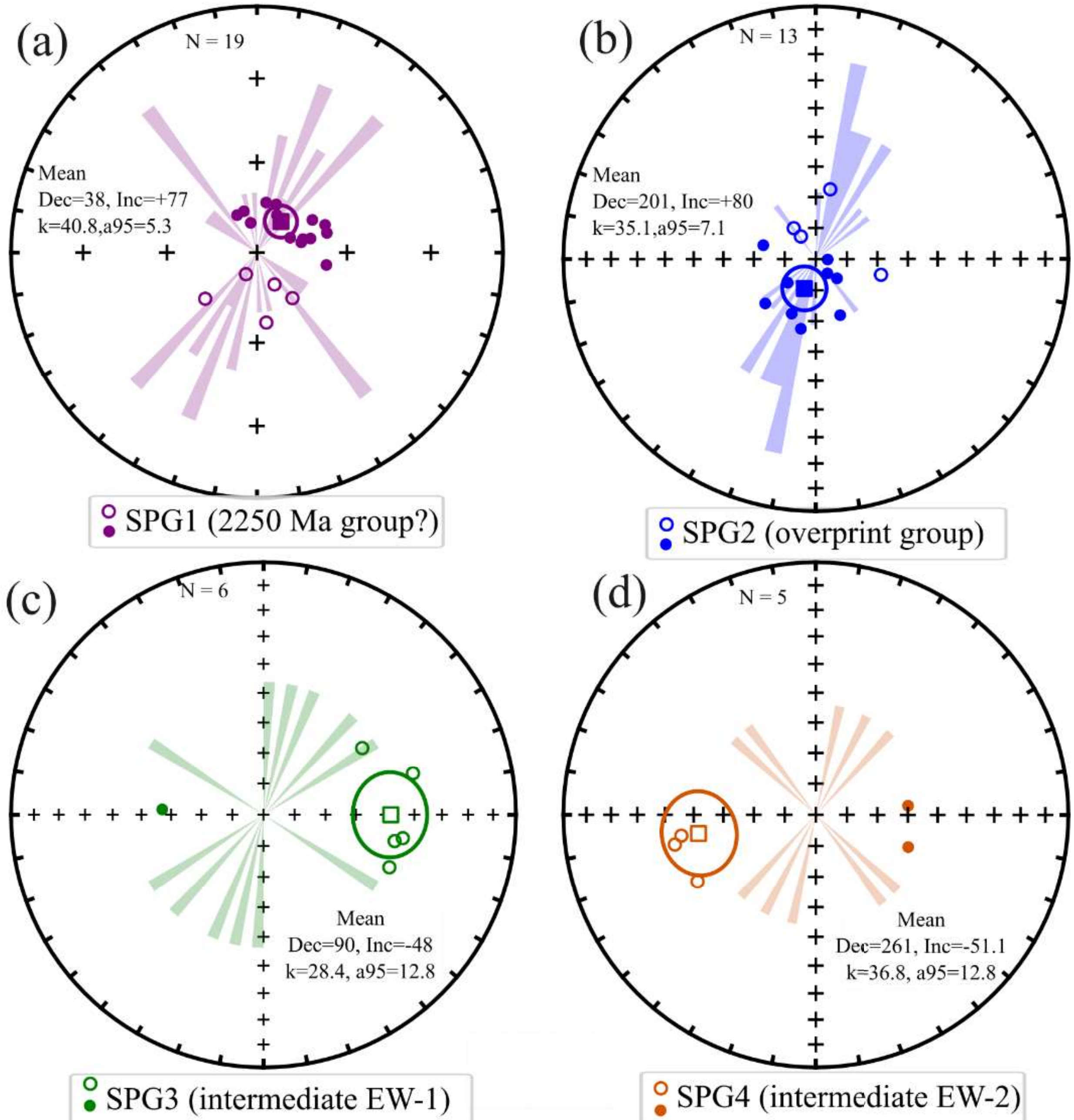

(a)
N = 19
Mean
Dec=38, Inc=+77
k=40.8,a95=5.3
SPG1 (2250 Ma group?)
(b)
N = 13
Mean
Dec=201, Inc=+80
k=35.1,a95=7.1
SPG2 (overprint group)
(c)
N = 6
Mean
Dec=90, Inc=-48
k=28.4, a95=12.8
SPG3 (intermediate EW-1)
(d)
N = 5
Mean
Dec=261, Inc=-51.1
k=36.8, a95=12.8
SPG4 (intermediate EW-2)

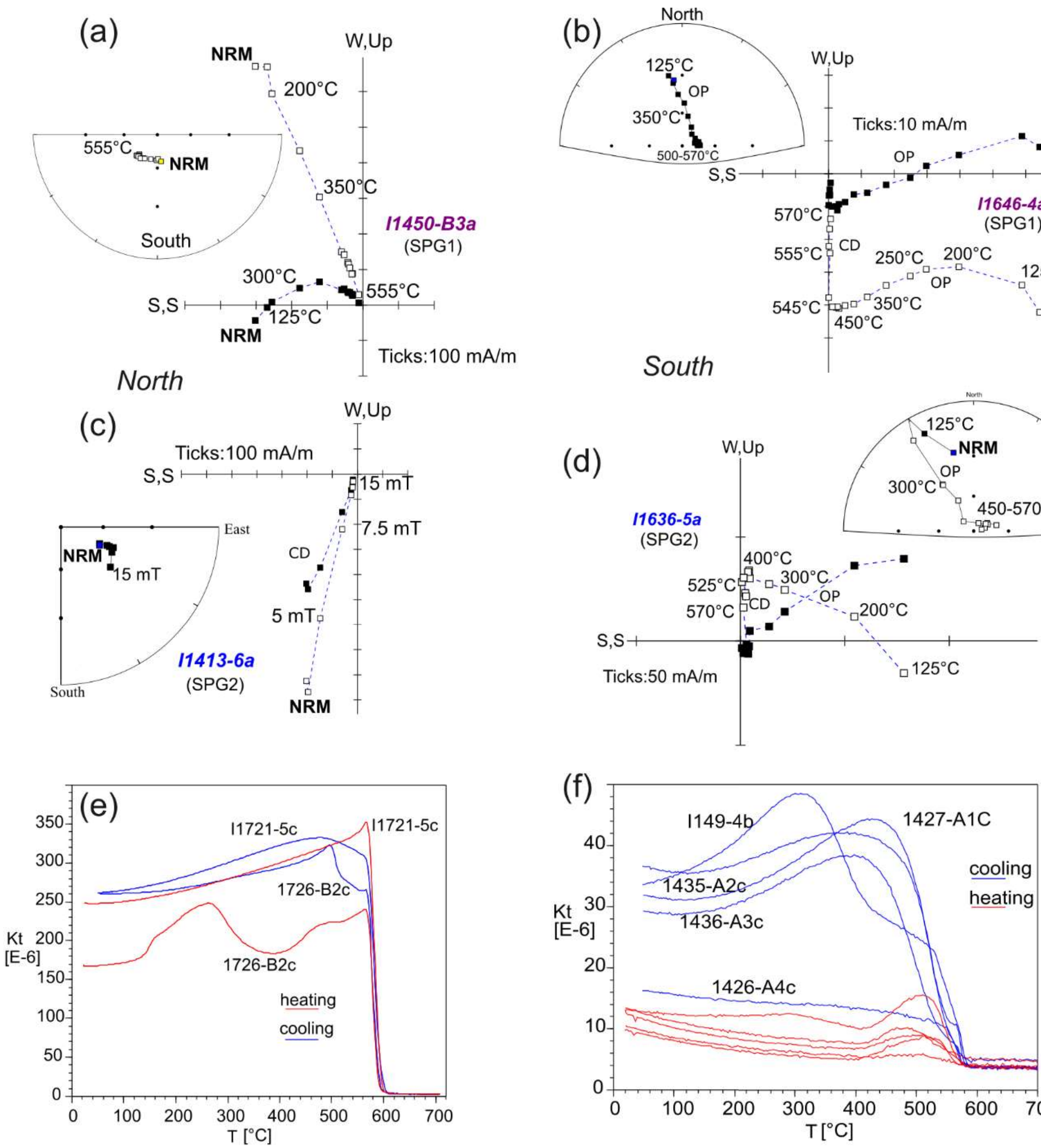
(a)
NRM
200°C
W,Up
555°C
NRM
350°C
South
I1450-B3a
(SPG1)
300°C
555°C
S,S
125°C
NRM
Ticks:100 mA/m
North
(b)
North
125°C
OP
350°C
500-570°C
W,Up
Ticks:10 mA/m
OP
S,S
570°C
I1646-4a
(SPG1)
555°C
CD
250°C
200°C
OP
125 °C
545°C
350°C
450°C
NRM
South
(c)
W,Up
Ticks:100 mA/m
S,S
15 mT
East
7.5 mT
CD
NRM
15 mT
5 mT
I1413-6a
(SPG2)
South
NRM
(d)
W,Up
North
125°C
NRM
OP
300°C
450-570°C
I1636-5a
(SPG2)
400°C
525°C
300°C
OP
570°C
CD
200°C
S,S
125°C
Ticks:50 mA/m
(e)
I1721-5c
I1721-5c
1726-B2c
Kt
[E-6]
1726-B2c
heating
cooling
T [°C]
(f)
I149-4b
1427-A1C
cooling
heating
1435-A2c
Kt
[E-6]
1436-A3c
1426-A4c
T [°C]

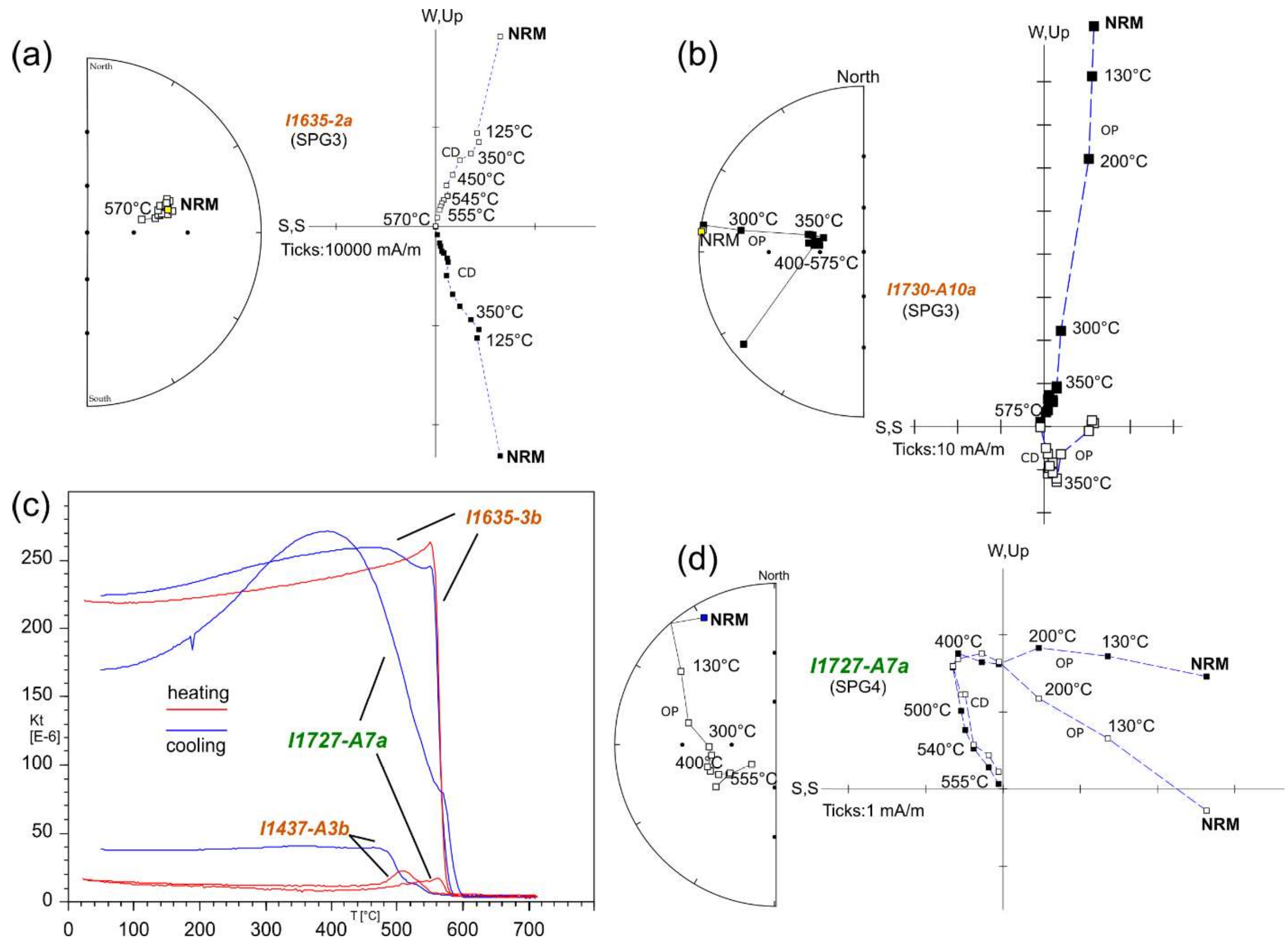

(a)
North
South
570°C
NRM
I1635-2a
(SPG3)
W,Up
NRM
125°C
CD
350°C
450°C
545°C
555°C
570°C
S,S
Ticks:10000 mA/m
CD
350°C
125°C
NRM
(b)
North
300°C
350°C
NRM
OP
400-575°C
I1730-A10a
(SPG3)
W,Up
NRM
130°C
OP
200°C
300°C
350°C
575°C
S,S
Ticks:10 mA/m
CD
OP
350°C
(c)
I1635-3b
heating
cooling
Kt
[E-6]
I1727-A7a
I1437-A3b
T [°C]
(d)
North
NRM
130°C
OP
300°C
400°C
555°C
W,Up
I1727-A7a
(SPG4)
400°C
200°C
130°C
NRM
OP
200°C
CD
500°C
130°C
OP
540°C
555°C
S,S
Ticks:1 mA/m
NRM

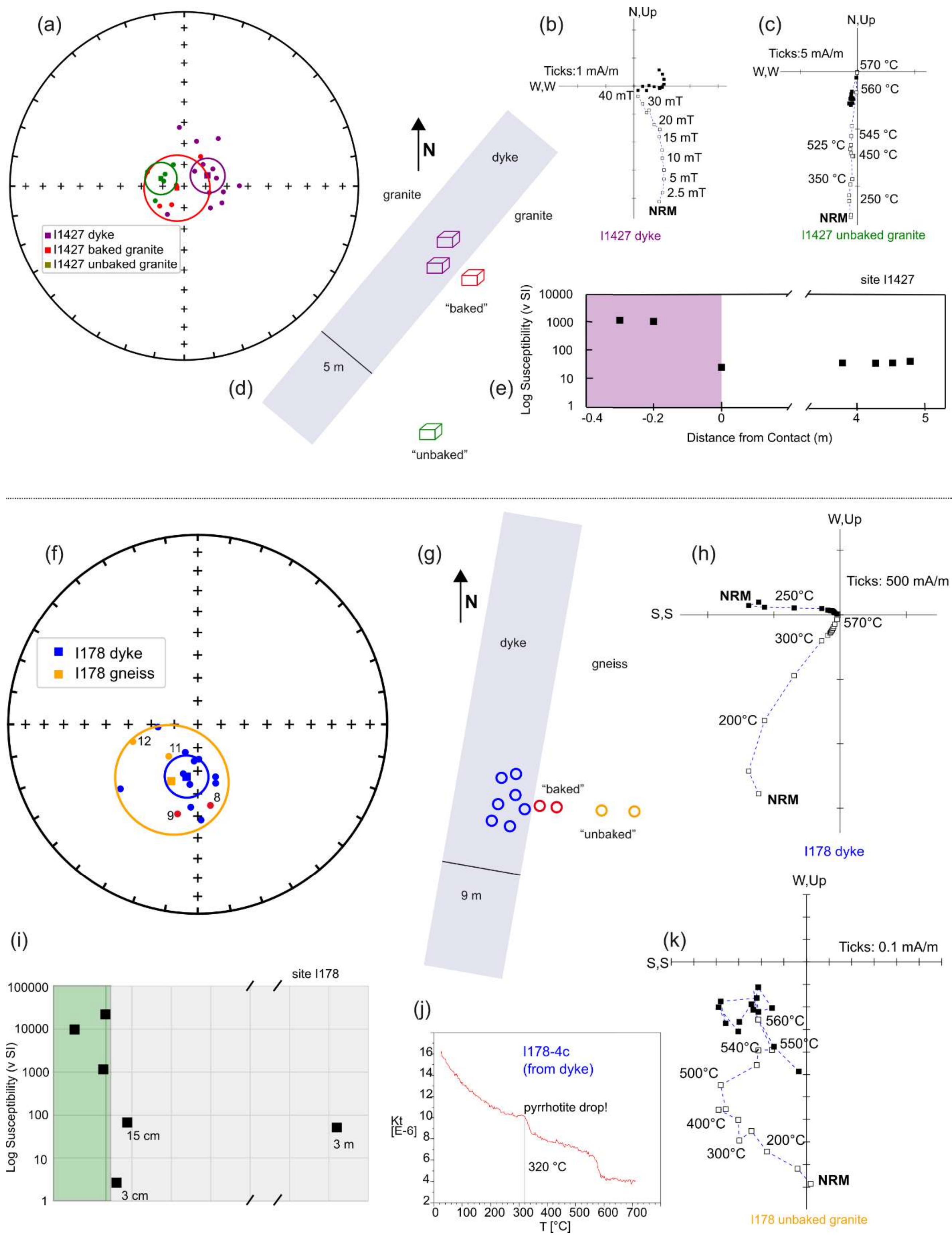

(a)
I1427 dyke
I1427 baked granite
I1427 unbaked granite
(b)
N,Up
Ticks:1 mA/m
W,W
40 mT
30 mT
20 mT
15 mT
10 mT
5 mT
2.5 mT
NRM
I1427 dyke
(c)
N,Up
Ticks:5 mA/m
W,W
570 °C
560 °C
545 °C
525 °C
450 °C
350 °C
250 °C
NRM
I1427 unbaked granite
N
dyke
granite
granite
"baked"
5 m
(d)
"unbaked"
(e)
site I1427
Log Susceptibility (v SI)
10000
1000
100
10
1
-0.4
-0.2
0
4
5
Distance from Contact (m)
(f)
I178 dyke
I178 gneiss
12
11
8
9
(g)
N
dyke
gneiss
"baked"
"unbaked"
9 m
(h)
W,Up
Ticks: 500 mA/m
NRM
250°C
S,S
570°C
300°C
200°C
NRM
I178 dyke
(i)
site I178
Log Susceptibility (v SI)
100000
10000
1000
100
10
1
15 cm
3 cm
3 m
(j)
I178-4c
(from dyke)
pyrrhotite drop!
Kt
[E-6]
320 °C
T [°C]
(k)
W,Up
Ticks: 0.1 mA/m
S,S
560°C
540°C
550°C
500°C
400°C
200°C
300°C
NRM
I178 unbaked granite

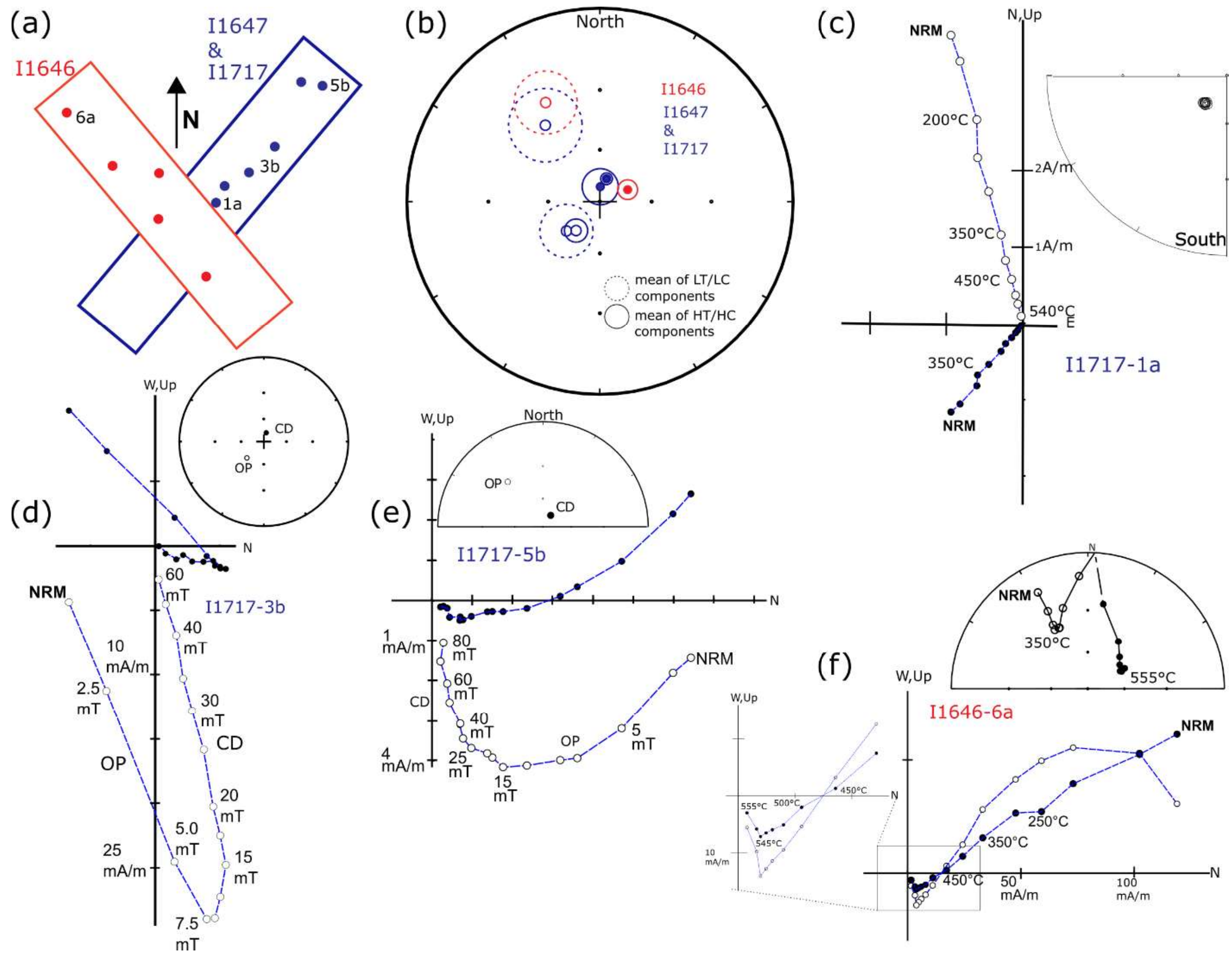

(a)
I1646
I1647
&
I1717
N
6a
5b
3b
1a
(b)
North
I1646
I1647
&
I1717
mean of LT/LC components
mean of HT/HC components
(c)
N,Up
NRM
200°C
2A/m
350°C
1A/m
450°C
540°C
South
350°C
NRM
I1717-1a
(d)
W,Up
CD
OP
N
60 mT
I1717-3b
NRM
40 mT
10 mA/m
30 mT
2.5 mT
CD
OP
20 mT
5.0 mT
25 mA/m
15 mT
7.5 mT
(e)
W,Up
North
OP
CD
I1717-5b
N
1 mA/m
80 mT
60 mT
CD
40 mT
25 mT
4 mA/m
15 mT
OP
5 mT
NRM
(f)
N
NRM
350°C
555°C
W,Up
I1646-6a
NRM
555°C
500°C
450°C
545°C
10 mA/m
250°C
350°C
450°C
50 mA/m
100 mA/m
N

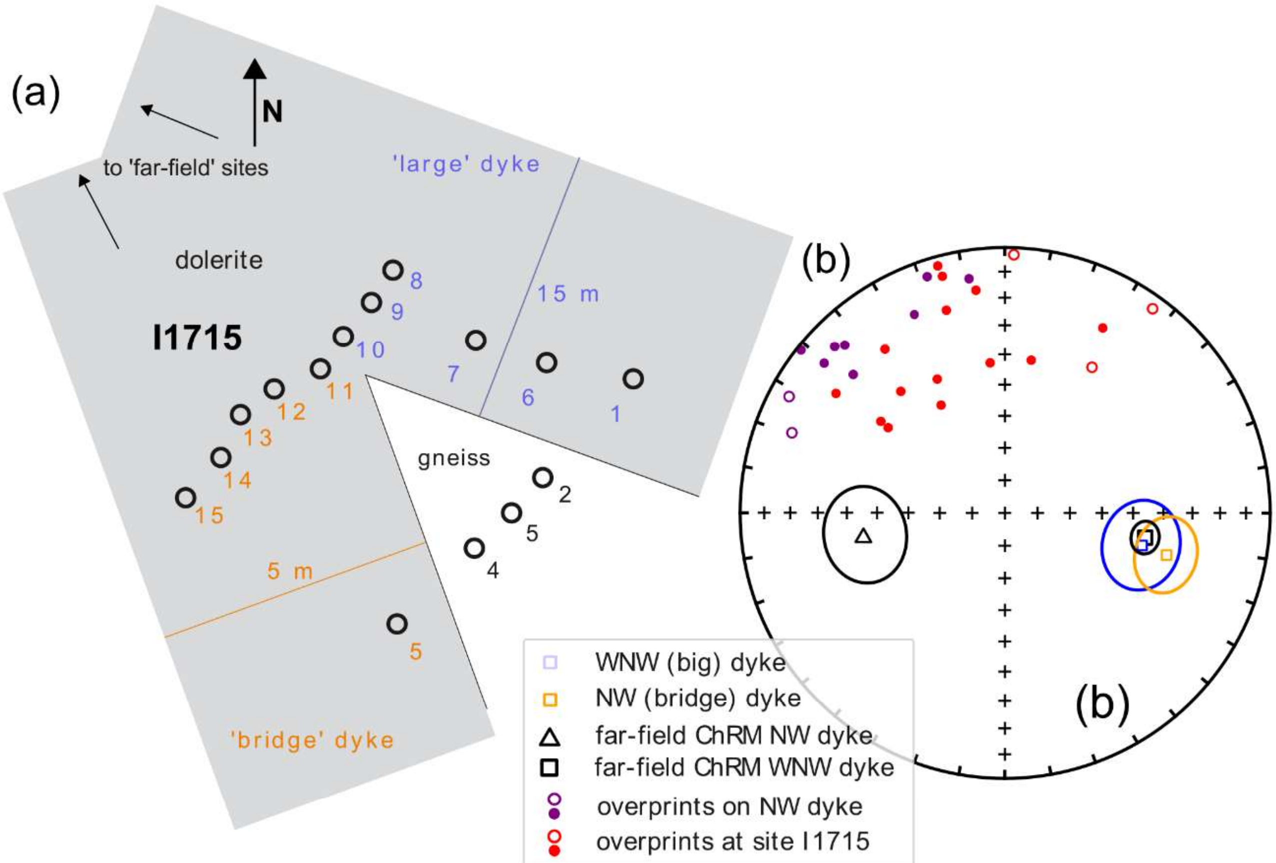
(a)
N
to 'far-field' sites
'large' dyke
dolerite
I1715
15 m
8
9
10
11
12
13
14
15
7
6
1
gneiss
2
5
4
5 m
5
'bridge' dyke
(b)
(b)
WNW (big) dyke
NW (bridge) dyke
far-field ChRM NW dyke
far-field ChRM WNW dyke
overprints on NW dyke
overprints at site I1715

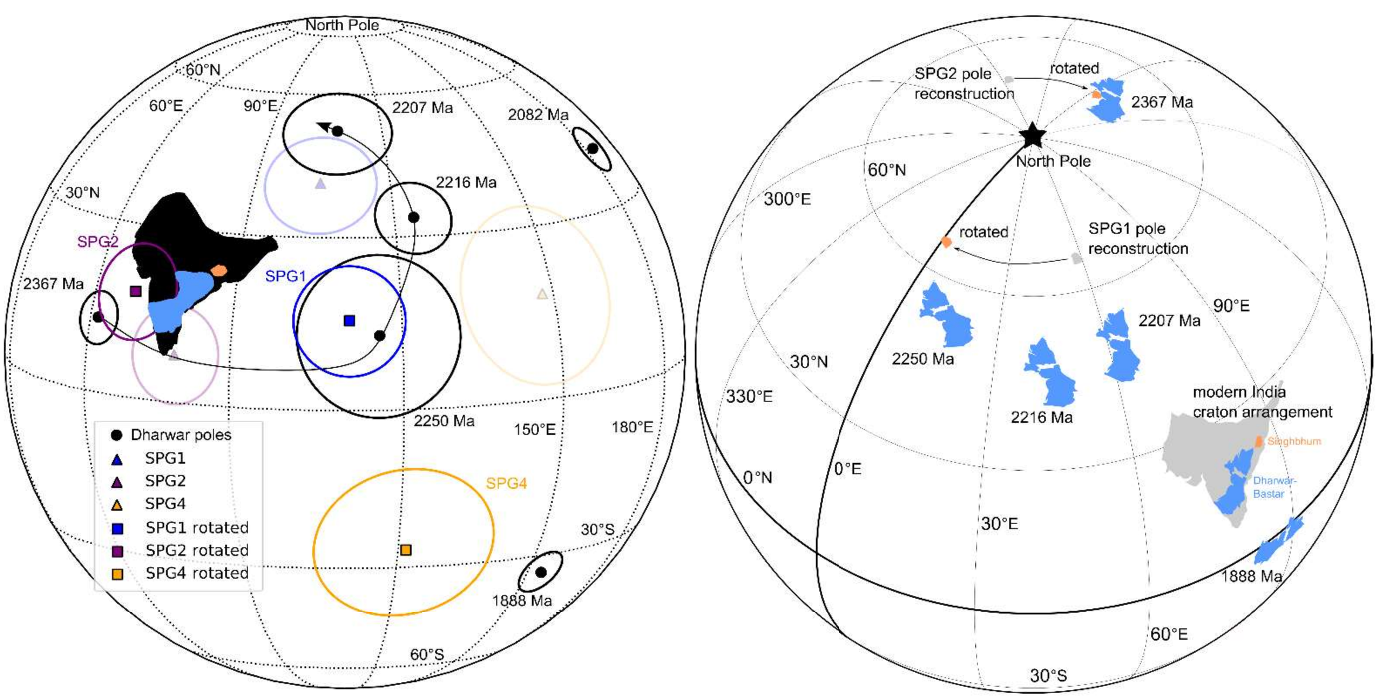
North Pole
60°N
60°E
90°E
2207 Ma
2082 Ma
2216 Ma
30°N
SPG2
2367 Ma
SPG1
2250 Ma
150°E
180°E
Dharwar poles
SPG1
SPG2
SPG4
SPG1 rotated
SPG2 rotated
SPG4 rotated
SPG4
30°S
1888 Ma
60°S
SPG2 pole reconstruction
rotated
2367 Ma
North Pole
60°N
300°E
rotated
SPG1 pole reconstruction
90°E
2207 Ma
30°N
2250 Ma
330°E
2216 Ma
modern India craton arrangement
Singhbhum
Dharwar-Bastar
0°N
0°E
30°E
1888 Ma
60°E
30°S

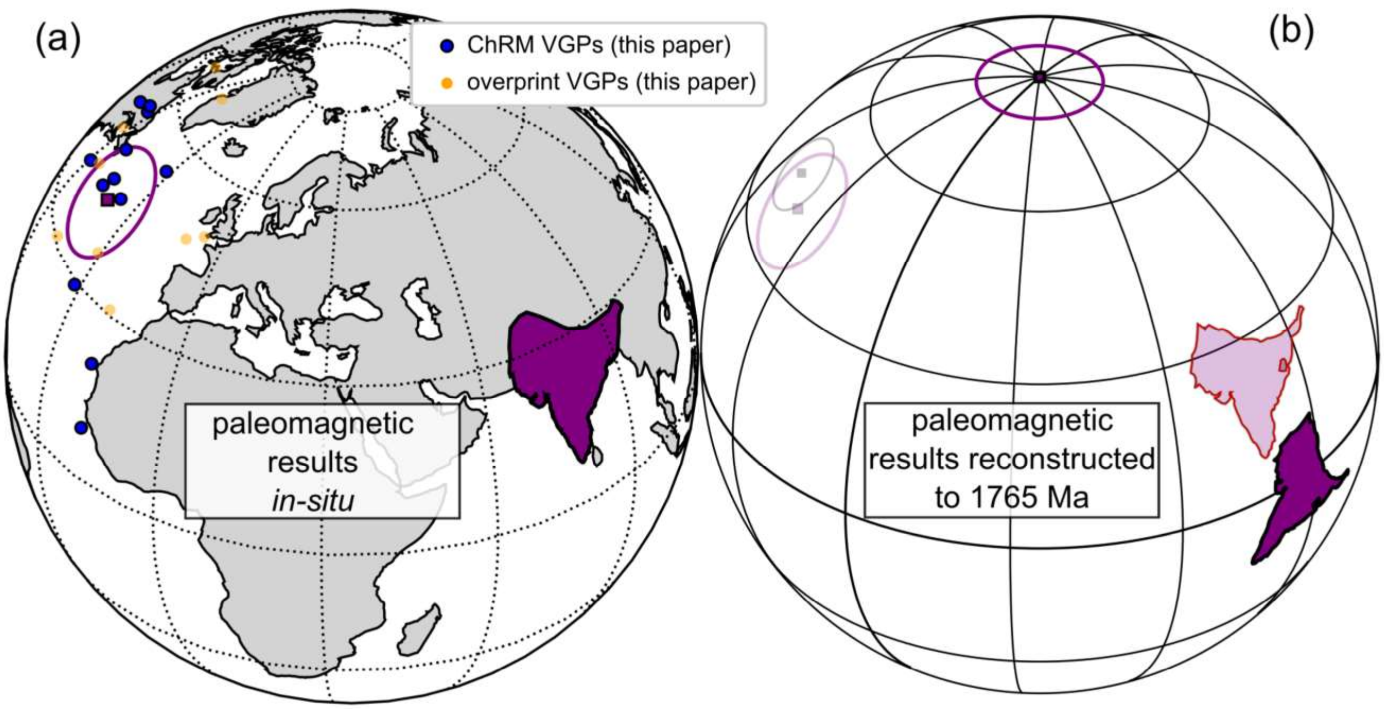

(a)
ChRM VGPs (this paper)
overprint VGPs (this paper)
paleomagnetic results *in-situ*
(b)
paleomagnetic results reconstructed to 1765 Ma

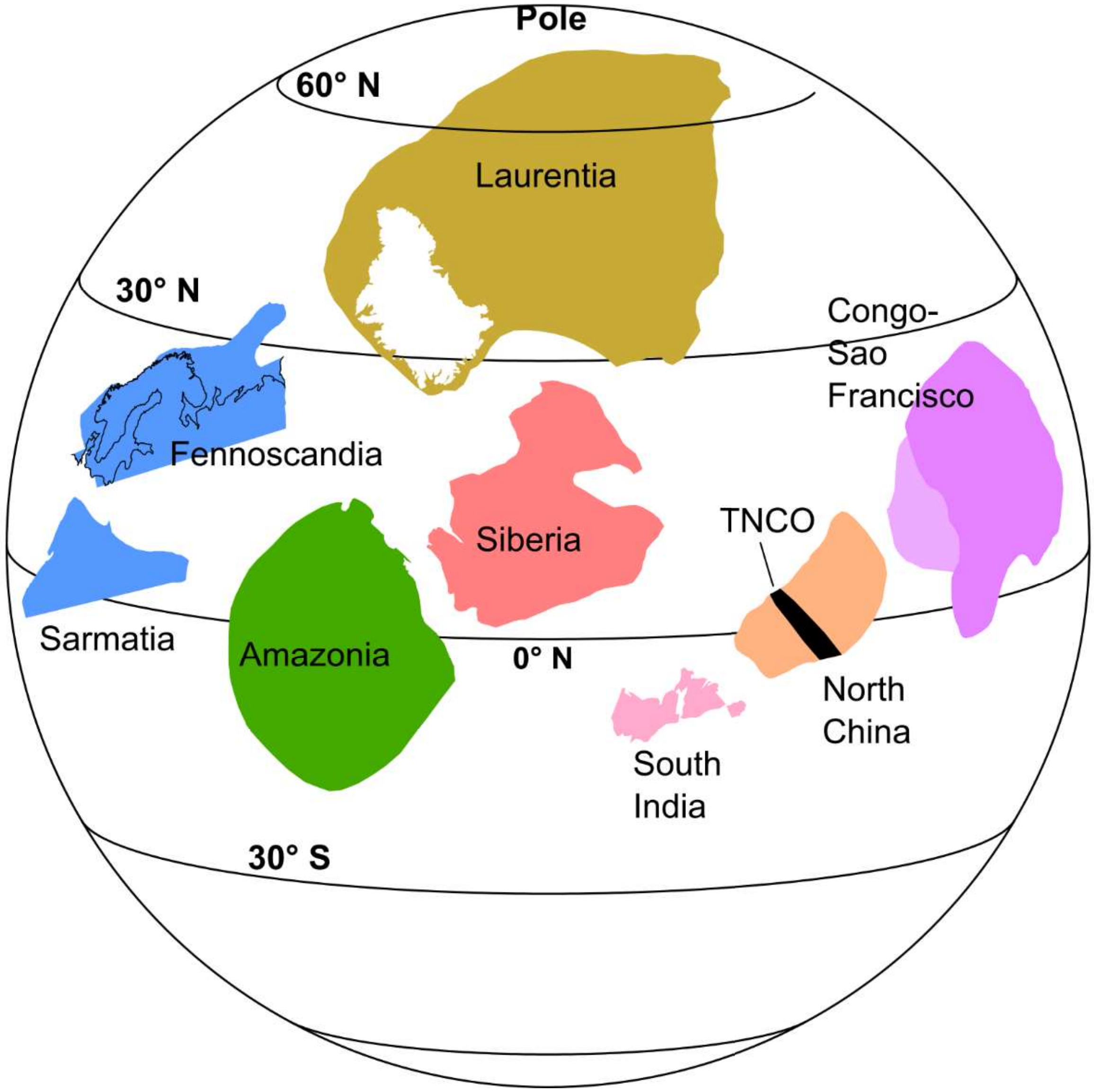

Pole
60° N
Laurentia
30° N
Congo-
Sao
Francisco
Fennoscandia
TNCO
Siberia
Sarmatia
Amazonia
0° N
North
China
South
India
30° S